Experimental Investigation on the Failure Mechanism for Critical Tube Diameter Phenomenon of Gaseous Detonations

Navid Mehrjoo

A Thesis
in
the Department
of
Mechanical and Industrial Engineering

Presented in Partial Fulfillment of the Requirements
for the degree of Doctor of Philosophy (Mechanical Engineering) at
Concordia University
Montréal, Québec, Canada

December 2014

CONCORDIA UNIVERSITY
SCHOOL OF GRADUATE STUDIES

This is to certify that the thesis prepared

By: Navid Mehrjoo

Entitled: Experimental Investigation on the Failure Mechanism for Critical Tube Diameter Phenomenon of Gaseous Detonations

and submitted in partial fulfillment of the requirements for the degree of

Doctor of Philosophy (Mechanical Engineering)

complies with the regulations of the University and meets the accepted standards with respect to originality and quality.

Signed by the final examining committee:

_____ Chair
Dr. J. Bentahar

_____ External Examiner
Dr. J.M. Bergthorson

_____ Examiner to Program
Dr. F. Haghighat

_____ Examiner
Dr. A. Dolatabadi

_____ Examiner
Dr. L. Kadem

_____ Thesis Supervisor
Dr. H.D. Ng

Approved by _____
Dr. A. Dolatabadi, Graduate Program Director

December 19, 2014

_____
Dr. Amir Asif, Dean
Faculty of Engineering and Computer Science

Abstract

Experimental Investigation on the Failure Mechanism for Critical Tube Diameter Phenomenon of Gaseous Detonations

Navid Mehrjoo
Concordia University, 2014

In this thesis, an experimental investigation is carried out to study the mechanism governing the successful transmission or failure on the critical tube diameter phenomenon when a fully developed, self-sustained detonation propagating in the confined tube transmits into an open space. The result of this study contributes to a better understanding of fundamental physical processes on the initiation, propagation and failure of the detonation.

To demonstrate the dependence of critical tube diameter d_c on combustion chemistry, two kinds of explosive mixtures are studied. The first is typical for common hydrocarbon mixtures characterized by irregular cellular structures and turbulent reactions zones. The other is referred to as stable mixtures particularly with combustibles highly-diluted with argon. A parametric study is carried out to measure critical tube diameters using stoichiometric acetylene-oxygen diluted with varying amount of argon to obtain these two types of mixtures. The present study validates that the well-accepted universal relation $d_c \approx 13\lambda$ holds for 0% - 30% argon diluted mixtures and breaks down when argon dilution increases up to 40%. Cell size measurement also indicates that the cellular detonation front starts to become more regular (or stable) when the argon dilution reaches above 40 - 50%. These results hence support that the physical process of critical tube diameter phenomenon is related to the stability nature of the detonation front and failure mechanism.

Failure mechanisms for the critical tube diameter phenomenon were previously postulated in the literature for the two kinds of mixtures. For unstable mixtures, the failure is based on the inability to form explosion centers in the failure wave when it has penetrated to the charge axis. For stable mixtures, the failure is caused by excessive curvature of the entire detonation front when the corner expansion waves have distributed the curvature over the diverging wave surface.

To discriminate between the two aforementioned modes of failure and clarify the importance of instability, two series of experiments are conducted: one by generating artificially small flow instability using small obstacles with different blockage ratios and the other by damping transverse instability using porous media to see how the critical tube diameter phenomenon responds to these perturbations. Results show that both generation and suppression of flow instability leads to a significant change in the critical condition for successful transmission. The critical pressure obtained in unstable mixtures is found lower with flow perturbation by the obstacles but adversely increases with the damping of instability using porous walled tube; while no noticeable effect could be observed in stable, argon-diluted mixtures.

The general implications of the present study are that in common unstable mixtures, instability is essential for the critical tube diameter problem and more generally, for the initiation and propagation of detonation, providing an efficient mechanism of gas ignition. For only a very special class of stable mixtures, the propagation of the detonation wave relies solely on the global coupling between the reaction front and the shock and instabilities only play a minor role on the dynamics of the detonation.

Acknowledgments

I would like to express my sincere gratitude to my supervisor Professor Hoi Dick Ng for his excellent guidance, caring, motivation, enthusiasm, immense knowledge and providing me with an excellent atmosphere for doing research. His expertise and understanding added considerably to my graduate experience. His patience and support helped me overcome many crises and finish this dissertation.

A very special thanks goes out to Professor John Lee, without whose motivation and encouragement I would not have considered a graduate career in this field of study. Professor Lee is the one teacher who truly made a difference in my life. He provided me with direction, technical support and became more of a mentor and friend, than a professor. It was though his, persistence, understanding and kindness that I completed my graduate degree. I doubt that I will ever be able to convey my appreciation fully, but I owe him my eternal gratitude.

Last but not the least, I would like to thank my beloved wife and best friend, Shooka, to whom this dissertation is dedicated to. None of this would have been possible without her support, concern, encouragement, and strength.

Table of Contents

List of Figures

List of Tables

Glossary

a	Sound speed
A_f	Frontal or projected area
C_p	Specific heat at constant pressure
C	Fitting parameter
C_D	Drag coefficient
D, d	Tube diameter
d_c	Critical tube diameter
d_{needle}	Needle diameter
E	Energy
F_D	Drag force
h_i	Specific enthalpy of specie i
L	Length
M	Mach number
N	Number of species
p	Pressure
t	Time
T	Temperature
u	Particle velocity
W	Molecular weight
y_i	mass fraction of specie i

Acronyms

BR	Blockage Ratio
CJ	Chapman-Jouguet
CFL	Courant - Friedrichs - Lax
FDS	Flux Difference Splitting
ID, OD	Inner or Outer Diameter
PDE	Pulse Detonation Engine
PLIF	Planar Laser Induced Fluorescence
TOA	Time-of-Arrival
ZND	Zel'dovich - von Neumann - Döring

Greek symbols

μ, α	Fitting parameters
Δ_I	Induction length
Δ_R	Reaction length
ε_I	Reduced activation energy
γ	Specific heat ratio
λ	Detonation cell size
τ	Chemical induction time
ρ	Density
χ	Stability parameter
$\dot{\sigma}$	Thermicity

Subscripts

i	i^{th} specie
I	Induction
max	Maximum
o	Initial condition, unburned mixture properties
R	Reaction

Chapter 1

Introduction

In general, a combustible mixture can support two modes of combustion wave. This division occurs according to the wave velocity, propagation mechanism, reaction sensitivity of the combustibles and hence, resulted in different change of thermodynamic state across it (Fickett and Davis 1979). For the slow combustion regime the wave is referred to as *deflagration* of which the propagation mechanism is governed mainly by diffusion. In this scenario, the wave propagates at typical velocities of the order of 1 m/s relative to the unburned gas. On the other limit, however, the violent mode of combustion is called *detonation*. At this extreme a self-sustained combustion-driven wave propagates at supersonic speed.

A thorough knowledge of the conditions under which detonations can be favorably initiated and their propagation can be sustained is of main concern to many industries. The ability to predict sensitivity of explosive mixtures, the initiation criterion, the conditions for transition from deflagration to detonation, and prediction of limits, are vital to the assessment, prevention and mitigation of accidental explosions in the chemical industries, coal mining and power production facilities (Ng and Lee 2008). Detonation theory also has practical application in new

propulsion systems development and understanding some interesting natural events. Pulsed detonation engines are examples of the practical use of detonation waves (Roy et al. 2004) or astrophysical detonation to explain the observation of supernovae (Oran 2005).

Although gaseous detonation waves have been studied extensively for many years, the development of successful theories for the prediction of practical properties in a given explosive mixture such as detonation limits, critical tube diameter or initiation energy (Lee 1984) remains a challenge. It is known that the ability to predict these dynamic parameters can only be resolved by thoroughly understanding the physical and chemical processes governing the initiation, propagation and failure of the detonation.

In the present thesis, the objective is to contribute to the understanding of the dynamics of detonation phenomenon in gaseous mixtures. This work is an experimental study of detonation dynamics aimed at understanding the instability of the front that results in different failure mechanisms under the losses condition in the critical tube diameters phenomenon. This research focuses on fully developed detonation waves propagating through a circular tube filled with a quiescent premixed, combustible gas and investigates their dynamics once the detonation emerges into an open space – a phenomenon known as the critical tube diameter problem. In this research, the purpose of the study is to answer the fundamental question of how a detonation fails and to improve our understanding of the nature of the instability and the governing physical and chemical processes on different dynamic parameters.

1.1 Classical Theory

The first attempt to theoretically explain the detonation phenomenon was formulated by Chapman, Jouguet, and Michelson in the late 19th century (Fickett and Davis 1979). By simplifying the detonation as a shock wave in which the energy release occurred instantaneously at its wave front and using a thermodynamic control volume, the well-known Chapman-Jouguet (CJ) theory allows the determination of its velocity and the equilibrium states across it and the results are typically found to agree quite well with experimental measurement. In the CJ theory, conservation equations on the upstream and downstream states together with the sonic condition are the only factors that are used in analyzing the detonation wave. Although it is possible to

predict the detonation state (e.g., detonation velocity, pressure, species concentration of products), the CJ theory provides no information for the chemical reaction rates in the chemical reaction zone or the actual non-equilibrium structure of the detonation. In order to describe various dynamic characteristics of the detonation phenomenon, e.g., initiation energy, detonability limits, detonation sensitivity of a combustible mixture, etc., what was most concerned was defining a model for the detonation wave structure in order to describe the transition zone across the wave. In other word, a model is needed to specify how the initial state transforms to the final state or the details within the control volume.

1.2 Detonation Structure

The classical model for the structure of detonation waves was first proposed in the early 1940's independently by Zel'dovich (1940), von Neumann (1942) and Döring (1943), hence referred to as the ZND model. The ideal ZND model describes a detonation wave to have a steady one-dimensional structure consisting of a leading shock wave followed by the chemical reaction zone. The combustible mixture is first compressed to a high temperature by the leading shock front and thereby, causing auto-ignition and initiating the chemical reactions after an induction time. Subsequent expansion of the high-pressure reacting gases provides the momentum change to sustain the propagation of the leading shock front. Despite its simplicity, the classical ZND model indirectly imposes a possible propagation mechanism for the detonation wave, i.e., auto-ignition by adiabatic shock compression. Another important application of the ZND model is that by defining a structure, it leads to the birth of a chemical length scale which can be considered to scale different detonation parameter from dimensional consideration.

Although the steady ZND model provides a basic structure of a detonation wave, the ideal assumptions far limit its degree of applicability to describe the experimentally observed detonation dynamics. In fact, the laminar steady structure described by the ZND theory is seldom observed experimentally. It has now been established, both theoretically and experimentally that almost all self-sustained detonation waves in common hydrocarbon combustible mixtures are inherently unstable leading to different unsteady and multi-dimensional features. Theoretically, hydrodynamic linear stability analyses (e.g., Erpenbeck 1964; Lee and Stewart 1990; Ng and Zhang 2012) have shown the ZND structure is always unstable to small perturbation (i.e., normal

modes having positive growth rates) with chemical and flow parameter values under real experimental conditions. Similarly, the observed detonation in real experiments using for example interferometry (White 1961) or Schlieren photography (Voitsekhovskii et al. 1958) usually has a cellular structure that consists of an ensemble of interacting shock waves sweeping back and forth across the detonation front. Their mutual interactions formed the equivalent triple point structure as in classical compressible fluid flows (Courant and Friedrichs 1946), defined by the Mach interactions of the transverse waves with the normal leading shock front. Various instabilities in the flow field associated with the chemical energy release also generate disturbances that act back on the detonation front and cause the propagation to be unsteady and multi-dimensional. The unsteady detonation structure can also be seen using a soot-foil technique (Lee 2008; Strehlow 1969). The technique relies upon the ability of the triple point shock interactions (with high shear) to etch their path on a surface coated with carbon soot deposit. The trajectories of these triple points, as recorded on the smoked foil as the detonation propagates by, have a characteristic fish scale or cellular pattern, see Fig. 1.1.

Figure 1.1 A smoked foil showing the characteristic fish scale in C_2H_2 + 2.5 O_2 +70%Ar at P_o = 12 kPa.

Because of its complex spatial-temporal unstable structure, direct measurements of detonation waves remain very difficult to conduct even with modern experimental diagnostics (Shepherd et al., 2002) and are usually limited to the analysis of the gross features appearing on soot foils (Schelkin & Troshin, 1965, Strehlow & Biller, 1969). Theoretically, the multi-scale nature of the detonation restricts any mathematical analysis such as asymptotic analysis or linear stability analysis to only simple models with simplified chemical kinetic rate laws which are far from realistic chemistry (Powers 2006; Ng and Zhang 2012). Although today's numerical simulations provide the full nonlinear instability of one- or two-dimensional detonation structures, interpretation or analysis of the numerical results requires better approaches. The

numerical resolution issues restrict the simulation to be performed only in small domains and a high-resolution three-dimensional simulation with detailed chemistry remains a challenge.

1.3 Detonation Dynamics Parameters

All detonation waves in gases are experimentally observed to be unsteady and multi-dimensional. Hence, the first step to understand the dynamics of detonations is to study all parameters that are responsible for characterizing a detonation wave. For an explosive mixture, the detonation properties are classified into two categories of equilibrium and non-equilibrium parameters. Equilibrium parameters are referred to those based on thermodynamics which can be predicted from the classical Chapman-Jouguet theory. CJ detonation pressure, temperature and CJ detonation velocity are some examples for the equilibrium parameters to provide some indication of the strength of the detonation. These equilibrium parameters differ from the category of non-equilibrium parameters in the sense that the structure of a detonation wave cannot be characterized. The non-equilibrium or "dynamic" detonation parameters are the parameters that are responsible for description of the non-equilibrium chemical kinetics, and instability processes involving the coupling between gas dynamics and thermo-chemistry. Therefore, dynamic parameters have some information that is needed to understand this structure. Detonation cell size, critical initiation energy and critical tube diameter are among the key dynamic detonation parameters. In fact, analyzing the variation of these aforementioned parameters provides more insight on the dynamics of detonation and is equivalent to studying the origin of the cellular patterns, the response of the detonation wave to strong perturbations of its cellular structure or observing how the detonation structure disintegrates near the failure limits or is formed under favorable initiation conditions.

1.3.1 Detonation cell size and definition of "stable" and "unstable" mixtures

The most commonly used dynamic parameter is the *characteristic cell size* of the detonation front, λ. The detonation cell size λ is an averaged characteristic length scale on the order of 1-300 mm for gaseous fuel-oxygen-diluent mixtures that can be measured using the smoked-foil technique, i.e., when a detonation passes over a lightly sooted surface, a pattern is left scoured in

the soot. The “fish-scale” or cellular pattern basically tracks the triple point trajectory as discussed in the previous section. Figure 1.2 shows again a typical smoked foil.

The cell size λ is a characteristic feature of the detonation front and it is found to relate to the detonation sensitivity of the mixture. The cell would be in smaller size for the sensitive mixtures, i.e., easy to initiate. In order to quantify the detonation structure, the very first step is to measure the cell size. The most suitable way of determining λ is by direct experimental measurement (smoked-foil record). However, for most commonly used hydrocarbon mixtures without dilution, the case would be complicated due to the fact that this pattern is often highly irregular, for example see Fig. 1.3. The experimental determination of the averaged cell size value is very subjective to personal judgment and some times, the uncertainty can be as big as a factor of 2.

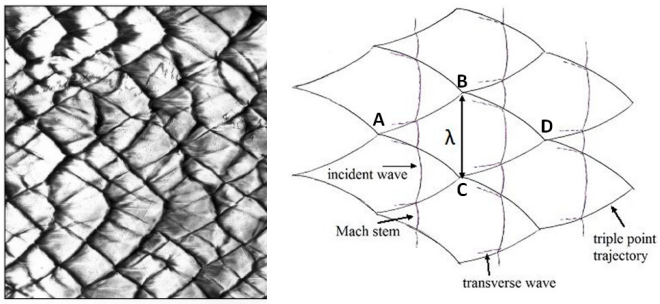

Figure 1.2 Some sample smoked foils and a schematic of the detonation front motion.

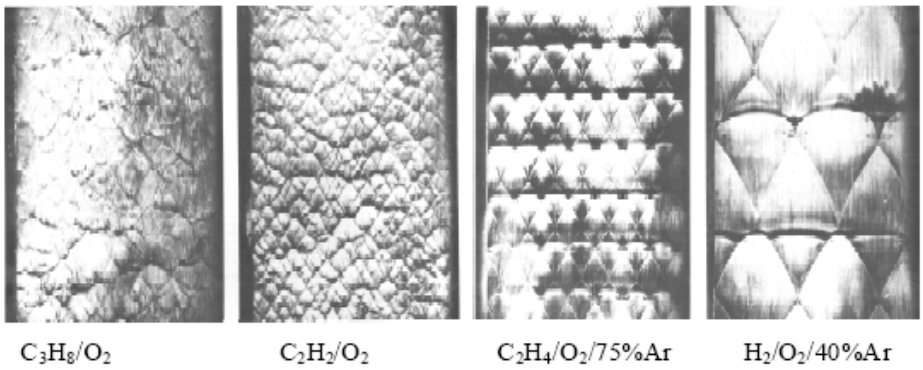

Figure 1.3 Experimental smoked foils for different types of combustible mixture (Voitsekhovskii et al. 1958).

It has become clear that characteristics of the cellular detonation front are strongly influenced by the chemistry of the reactive mixture. Experimentally, it is shown the cell regularity of detonations is dependent on the chemical systems, which can undergo different chemical reactions with different kinetics. As Strehlow (1969) pointed out, significant differences on the

cellular structure can be observed in mixtures with different chemical composition. For example, as seen already in Fig. 1.3, sensitive mixtures like H_2-O_2 or high temperature systems such as fuel-oxygen mixtures highly diluted with a monotonic gas such as argon are generally observed to produce remarkably regular or more organized cellular pattern having weak transverse waves and a piece-wise laminar frontal structure. These types of mixtures are usually referred to as "stable" mixtures. However, for common hydrocarbon fuel-oxygen mixtures such as CH_4-O_2 or fuel-air mixtures without dilution, the cell patterns recorded on the smoked foil can be extremely irregular or disorganized and the detonation structure consists of strong transverse waves. Such evidences are recently revealed by Austin et al. (2005) using the PLIF technique to visualize the detonation front structure as shown in Fig. 1.4. These mixtures are typically classified as "unstable mixtures".

Remark: It is important to note that in this thesis *the stability of the detonation front is described by the regularity of the cell size pattern and level of fluctuation embedded in the detonation front structure.*

Detonations with regular structure appear to have distinctly different macroscopic behavior than those with irregular structure and dynamics parameters all appear to scale differently. In this research, we consider a number of fuel-oxidizer systems that are representative of fronts of two extremes: highly unstable and stable detonations. A critical question that should be addressed is: *how the nature of instability affects the macroscopic behavior of the detonation waves?*

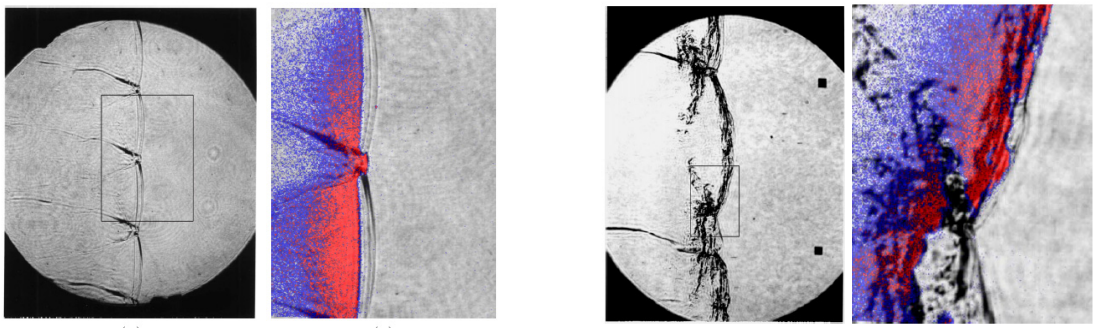

Figure 1.4 Images of a) stable detonation front propagating from left to right in $2H_2+O_2+12Ar$ mixture; and b) highly unstable detonation front propagating from left to right in $C_2H_4+3O_2+10.5Ar$ mixture at p_o = 20 kPa. i) Schlieren; and ii) superimposed Schlieren and fluorescence OH PLIF image (Austin et al. 2005).

1.3.2 Critical energy for direct initiation of detonation

The question of how a detonation is initiated can be tackled through the study of the well-defined problem of direct blast initiation, where the detonation is resulted from the decay of a strong point blast wave generated by a concentrated energy source (Lee and Higgins 1999). The successful initiation should depend on the condition to achieve proper coupling between gasdynamics and chemical reactions. Equivalently to the classical blast wave theory where the source energy is the sole parameter that governs the decay of a point spherical blast (Taylor 1950), the suitable dynamic parameter to characterize the detonation initiation process is the *critical energy* for direct initiation.

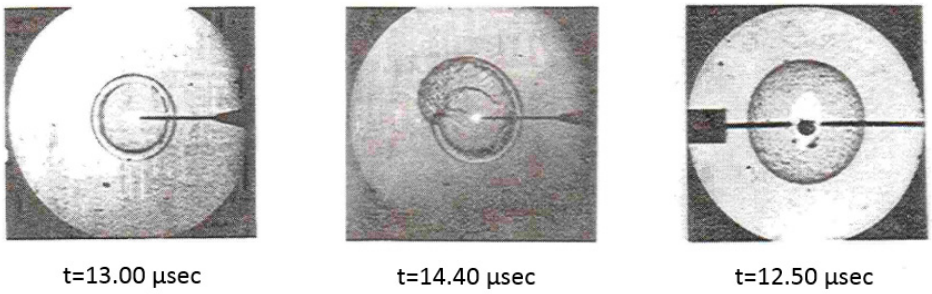

a) Subcritical regime b) Critical regime c) Supercritical regime

Figure 1.5 Different regime of direct initiation of detonation (Bach et al. 1969).

This parameter indicates that a specific amount of energy is needed to initiate a detonation by considering initial conditions for a particular mixture. The reaction zone and the blast front will be decoupled as it starts decaying in the condition where the igniter energy is less than its critical value, see for example, Fig. 1.5.

Despite the fact that there exist a lot of experimental studies in the literature to measure the critical initiation energy of direct detonation initiation, discrepancies remain. Generally, it is not easy to determine this energy due to the fact that its value depends on the initiation method (e.g., high voltage discharge, ignition wire, blast cap, condensed explosive, etc.). For instance, the igniter geometry, its material, and energy-time characteristics are some of the parameters that control the amount of initiation energy delivered to a specific mixture.

In spite of all the efforts in the past decades toward the understanding of direct initiation of detonation, a quantitative predictive theory from first principles based on thermo-chemical and

chemical kinetic data of the mixture for the critical energy, i.e., minimum energy required for successful initiation, is also not yet available. Theoretically, existing models are mostly developed based on the empirical hypothesis from the pioneering work of Zel'dovich et al. (1957), which states that for spherical detonations the decay time of the initiating blast wave must be of the order of the induction time when it has reached the Chapman-Jouguet strength and the critical energy E_o can be scaled with the chemical induction time τ (i.e. $E_o \sim \tau^3$). This scaling criterion does not take into account the dynamics of the event. A better scaling may perhaps be achieved by $E_o \sim \lambda^3$ where λ is the cell size value, representing better the dynamics of the detonation structure. However, the uncertainty involved the cell size determination makes this correlation undesirable – any uncertainty in cell size value will be magnified by a power of 3.

1.3.3 Critical tube diameter

The critical tube diameter phenomenon has long been a classical problem in detonation research. It not only provides a well-defined fundamental problem in understanding both initiation and failure of detonation waves, but knowledge of the critical tube diameter also has practical applications such as in the design of initiators for pulse detonation engines, e.g., when the detonation transmits from the small pre-detonator to the main thrust tube of the pulse detonation engine (Kailasanath 2003). The critical tube diameter, D_c, is defined as the minimum diameter of a round tube for which a detonation emerging from it to an open space can continue to propagate. If $d < d_c$, the detonation will quench and cannot transmit into the free space (Lee 1984, 1996), see Fig. 1.6. This parameter is perhaps the most accessible and accurately measurable parameter that describes the dynamic behavior of a combustible. At specific initial conditions, this parameter has a rather unique value for a given detonable mixture. The critical tube diameter can thus be considered as an alternative length scale that provides an assessment of the relative detonation sensitivity of combustible mixtures. This scale is in contrast to the detonation cell width which, while a fundamental length scale of the detonation structure, can present significant variability when measured. The critical diameter problem contains also all fundamental mechanisms of failure and initiation.

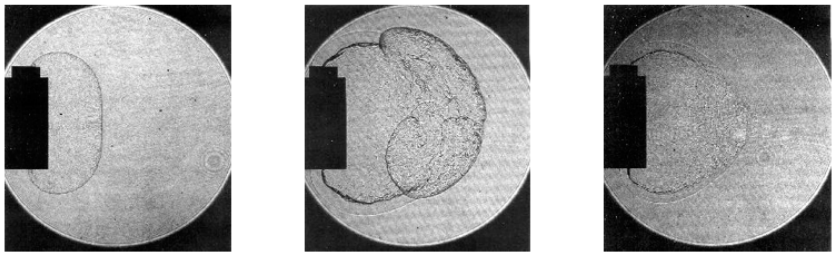

Figure 1.6 Detonation diffraction experiments by E. Schultz (2000): (a) super-critical (successful) detonation diffraction regime; (b) near-critical diffraction; (c) sub-critical (quenched) detonation diffraction regime.

Although in literature there is an abundant amount of measurement of detonation dynamic parameters since 1960's, there remain some key gap and possible future research. Among the three detonation dynamic parameters, cell sizes data are the most abundant one and values from different studies are well tabulated in the CALTECH detonation database (1997). Similarly, critical initiation energy for a number of combustible mixtures was also measured by many researchers. Recently, a systematic approach and a new set of data for a wide range of hydrocarbon mixtures were published (Zhang et al. 2011a, 2011b, 2012a, 2012b, 2012c, 2013). Unlike these two parameters, critical tube diameter data are rather scarce. There is a need to obtain more measurement of critical tube diameter for a number of different mixtures.

For all the dynamic parameters discussed above, until now there is no universal theory from first principles for predicting their values. Lack of the complete understanding of the physical processes that leads to these phenomena will be the key ingredient to develop rigorous theories for the detonation dynamic parameters. To better describe the dynamics of detonations, the physics of the critical tube diameter phenomenon is believed to provide the key issue for the understanding of the general physical mechanisms governing detonation propagation and failure.

1.4 Failure Mechanisms for the Critical Tube Diameter

From the literature on the critical tube diameter problem, it was found that the critical tube diameter d_c for many common hydrocarbon fuels-oxygen or -air mixtures is universally about 13 detonation cell widths of the mixture (i.e., $d_c \approx 13\lambda$) (Mitrofanov 1965; Knystautas et al. 1982). However, recent experiments have shown this correlation begins to be invalid for some special

cases of highly "stable" mixtures with argon dilution where the critical conditions can vary as much as $d_c \sim 20$ to 30λ (e.g., Shepherd et al. 1986; Moen et al. 1986; Desbordes et al. 1993). It is long suggested that this effect is resulted from the instability nature or difference in regularity between the detonation fronts in undiluted (unstable) and diluted (stable) mixtures. As shown in the earlier Section 1.3.1 that for undiluted hydrocarbon mixtures, typically with high activation energy in the chemical reaction (thus high reaction sensitivity), the cellular detonation front is unstable embedded with small scale instabilities and its propagation relies on the interactions of transverse waves (Shepherd 2009; Radulescu 2003). On the other hand, for detonations in combustible mixtures that have been highly diluted with argon, the detonation front is very regular or appears to be piece-wise laminar where cellular instabilities that do not seem to play a prominent role on the propagation of a stable detonation (Radulescu et al. 2002). The ZND structure becomes more valid and a stable, ZND detonation relies on the classical mechanism of shock-induced auto-ignition.

In 1996, Lee has proposed the two modes of failure consisting of one by a local failure mechanism that is linked to the effect of instabilities for undiluted mixtures, and the other due to the excessive curvature of the global front in mixtures highly diluted with argon. In Lee's conjecture the significant difference of the critical tube diameter phenomenon in mixtures with regular and irregular cellular structure is due to the different mechanism of detonation failure.

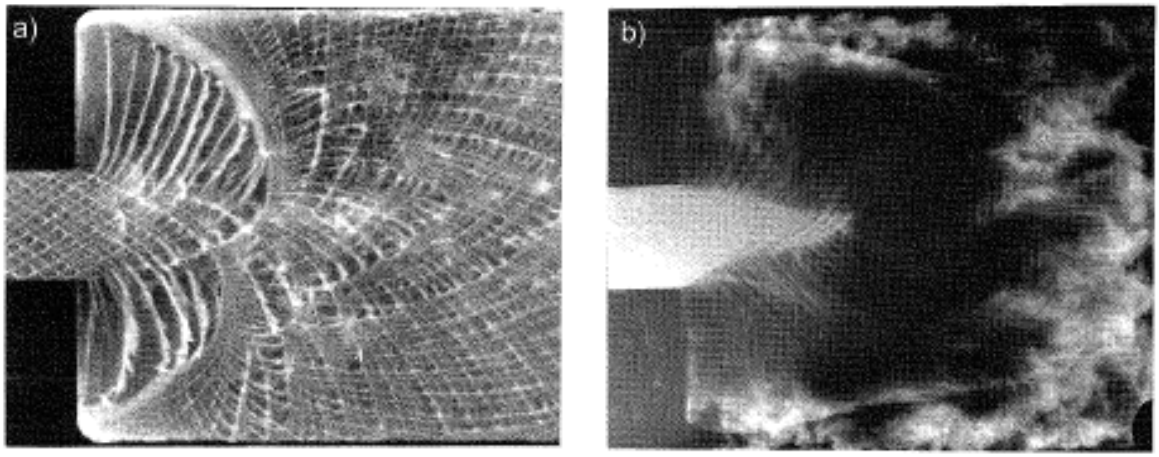

Figure 1.7 Open shutter photographs showing the critical tube diameter phenomenon in a) unstable and b) stable gaseous mixtures.

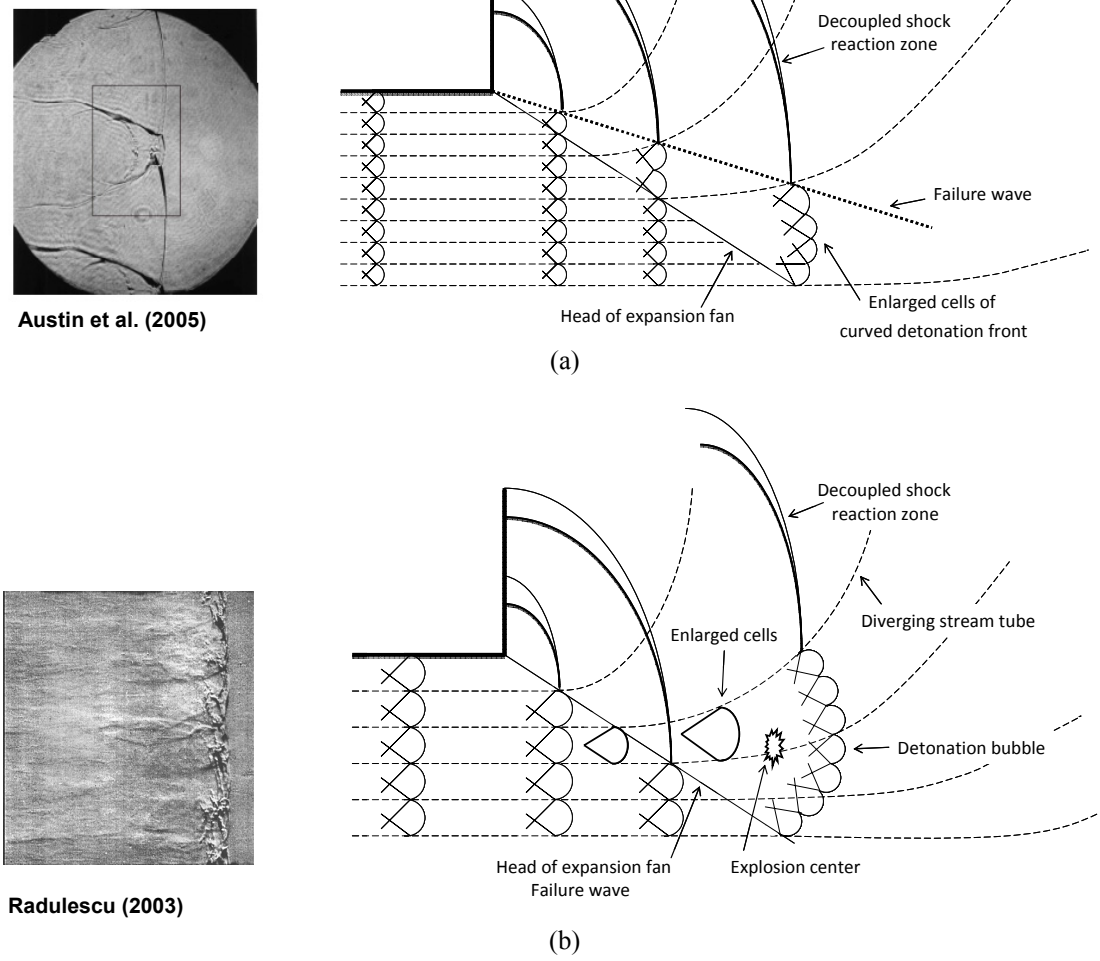

Figure 1.8 A schematic illustrated the two postulated failure mechanisms for a) stable and b) unstable explosive mixtures.

By analyzing the open-shutter photographs by Vasil'ev as shown in Fig. 1.7, Lee pointed out that for unstable detonations, successful transmission is invariably found to originate from localized region in the failure wave, which eventually amplified to sustain the detonation propagation front in the open area. Hence, failure is linked to the suppression of instabilities at which localized explosion centers are unable to form in the failure wave when it has penetrated to the charge axis. While for stable detonations failure is predominantly caused by excessive curvature of the entire detonation front, whereby the corner expansion waves distribute the curvature over the detonation surface. In more details, for stable (regular cellular structure)

detonations where local instabilities were substantially absent, propagation is as a result of the shock compression described by the classical steady ZND model and the continuous energy release of bulk explosive gas as it converts into product. In other words, in stable mixtures, transverse waves play a negligible role on the propagation of the stable detonation. When the stable detonation emerges from a confined tube with a diameter less than critical diameter, the products are unable to keep the pressure behind the shock front due to extreme expansion at the edges resulted in a high curved front. The detonation fails due to the mechanism of excessive front curvature which leads to high velocity deficit and eventually the total decoupling between the leading front and the reaction zone. This mechanism is illustrated in Fig. 1.8a.

On the other hand, for unstable (irregular) detonations, strong transverse waves play a dominant role, and the unstable cellular structure is essential to the propagation of the detonation. In fact, the instability effect makes the detonation structure more robust. Lee argued that for an unstable detonation, the failure is caused by the inability to develop new cells via instability as the rarefaction waves penetrate into the detonation that governs failure. Although globally the detonation front can be quenched due to curvature, however, in unstable mixture localized fluctuation can give birth to explosion as shown in Fig. 1.8b and provide another mechanism for the transmission of the detonation in the unconfined region. In an empirical manner, to put in test of this theory, new critical tube diameter experiments are needed that could unambiguously discriminate between the two postulated mechanisms of failure.

1.5 Objective and Outline of the Present Study

In this research, the objective is to contribute to the understanding of detonation dynamics. The present study presents a detailed investigation of the classical problem of critical tube diameter phenomenon, particularly focusing on the failure mechanism and the effect of instability. This study allows one to look at how a detonation is attenuated and failure during the diffraction. In this study, a wide range of mixtures are investigated displaying different levels of cell regularity, ranging from "highly stable" such in C_2H_2-O_2-Ar mixtures to "highly unstable" mixtures such as C_2H_2-N_2O mixtures. From the literature review, it is clear that there is a lack of experimental data on the critical tube diameter problem. Although some conjecture has been

proposed to understand the criterion for successful transmission of a self-sustained detonation from a confined tube to an open area from the description of the failure during detonation diffraction, there still lacks of concrete evidence to demonstrate concretely the mechanisms responsible for detonation failure in highly regular mixtures due to excessive global curvature and in highly irregular undiluted mixtures invariably linked to the suppression of instabilities.

The present thesis is organized into the subsequent six Chapters. The general description of the experimental apparatus, the diagnostic used and the general experimental procedure are provided in Chapter 2. The effect of instability on the critical tube diameter problem is first investigated in Chapter 3 using stoichiometric C_2H_2-O_2 mixtures diluted with varying amount of argon. It is shown from previous studies that by increasing the amount of argon dilution, the detonation front can be rendered more "stable" and the structure becomes more "laminar". By systematically varying the amount of argon in the mixture and measure its critical tube diameter, the effect of instability on this dynamic parameter can be elucidated and the effect of the critical argon dilution can be revealed.

The subsequent Chapters are then presented to describe a series of experiments where their goals are to unambiguously discriminate between the two postulated modes of failure and the role of flow instability on the critical tube diameter problem in the two kinds of stable or unstable mixtures. In Chapter 4, needle obstacles are introduced near the exit of the confined tube before the detonation emerges into the unconfined space to look at how the detonation responds to the artificially generated flow perturbation in the critical tube diameter phenomenon. In Chapter 5, injectors based on the result of Chapter 4 are designed to facilitate the transmission of detonation from a small area to a larger one for practical application in propulsion system such as PDE. In contrast to the experiment using obstacles to induce flow disturbance, Chapter 6 presented the results where transverse instability is attenuated using porous walled section and see how the detonation responds to these suppressions towards the diffraction and transmission process. Finally implication of the results from each proposed experiment and conclusion on the important of instability or transverse wave on the propagation and failure of detonation waves is provided in Chapter 7.

1.6 Related Publications

Results presented in Chapter 3 form half part of the following published journal article where the critical tube diameter experiments presented is performed by the thesis author.

- Zhang B, Mehrjoo N, Ng HD, Lee JHS and Bai CH (2014) On the dynamic detonation parameters in acetylene-oxygen mixtures with varying amount of argon dilution. *Combustion and Flame* 161(5): 1390-1397.

Chapters 4 to 6 of the present thesis contain materials, which appear in the following peer-reviewed journal articles and the thesis author was the primary researcher in all these publications.

- Mehrjoo N, Zhang B, Portaro R, Ng HD and Lee JHS (2014) Response of critical tube diameter phenomenon to small perturbations for gaseous detonations. *Shock Waves Journal* 24(2): 219-229.
- Mehrjoo N, Portaro R and Ng HD (2014) A technique for promoting detonation transmission from a confined tube into larger area for pulse detonation engine applications. *Propulsion and Power Research* 3(1): 9-14.
- Mehrjoo N, Gao Y, Kiyanda CB, Ng HD and Lee JHS (2014) Effects of porous walled tubes on detonation transmission into unconfined space. *Proceedings of the Combustion Institute*, 35. In press. doi:10.1016/j.proci.2014.06.031

Chapter 2

Experimental Facility

The methodology used in the present thesis is experimental approach. This Chapter is therefore devoted to provide the detailed description of the experimental facility and procedure to conduct the present thesis investigation on the critical tube diameter problem. To demonstrate the reliability of the experimental apparatus, diagnostics and procedures, some benchmarks tests are conducted and compared with data published in the literature.

2.1 Experimental Apparatus

All the critical tube diameter experiments conducted in this thesis are carried out in the gaseous detonation facility located at the combustion and energy systems laboratory, Concordia University. A schematic of the general experimental apparatus for the measurement of the critical tube diameter is shown in Fig. 2.1. The setup is a modified high-pressure spherical chamber used previously for the measurement of critical energy for direct initiation of spherical

detonations (Kamenskihs et al. 2010; Zhang et al. 2011a, 2011b, 2012a, 2012b, 2012c, 2013). The chamber is 20.3 cm in diameter and has a wall thickness of 5.1 cm. The chamber's body is connected at the top to a 41.8-cm long vertical circular steel tube. In most cases, four different diameters of the tube D were considered, i.e., D = 19.1, 15.5, 12.7 and 9.13 mm. The tube diameter D was varied via inserting smaller diameter tubes.

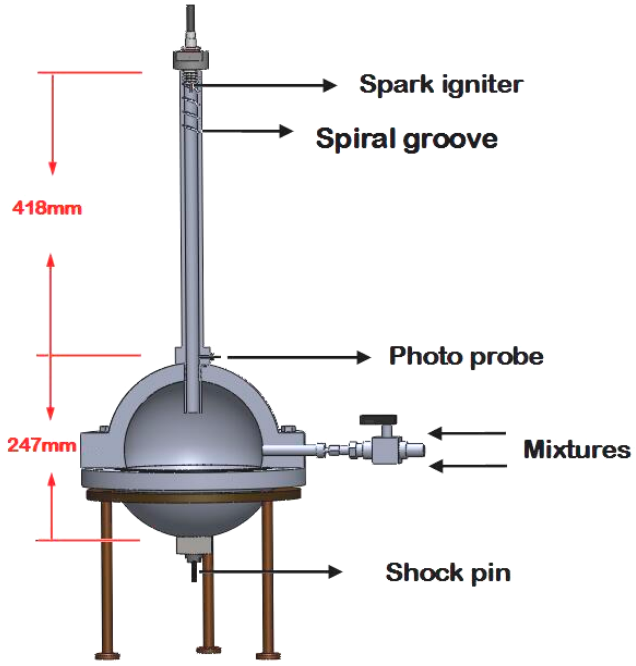

Figure 2.1 A schematic and photograph of the critical tube diameter experiment.

2.2 Measurement Diagnostics and Experimental Procedure

The explosive mixture was prepared beforehand in separate vessel by the common method of partial pressure. The gases were allowed to mix in the bottle for at least 24 hours in order to ensure mixture homogeneity for each tested mixture. For each experiment, the setup was initially evacuated to approximately 100 Pa and then filled through the valve with mixtures at various initial test pressures p_o. The initial pressure measurement was taken via an Omega model PX309-030AI pressure transducer (0–30 psi) with an accuracy of ±0.25 % full scale.

A planar self-sustained Chapman–Jouguet (CJ) detonation was initiated with a high-voltage spark ignition source shown in Fig. 2.2, which consisted of a high-voltage power supply,

capacitor bank, a gap switch, a trigger module (TM-11A, PerkinElmer Inc.) and a slender coaxial electrode mounted at the top of the vertical steel tube (Kamenskihs et al. 2010). The self-sustained detonation is subsequently transmitted into the relatively larger spherical chamber.

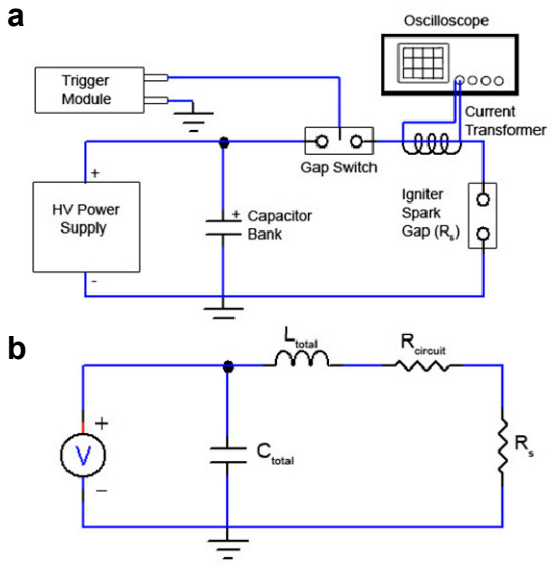

Figure 2.2 a) The ignition circuit components; and b) its equivalent RLC circuit diagram.

A photo probe and a piezoelectric shock pin (CA-1136, Dynasen Inc.) were mounted at the top and bottom of the spherical bomb, which were used to record the time-of-arrival (TOA) signals of the wave onto the oscilloscope (Rigol Digital Oscilloscope 100MHz DS1102E). From the TOA between initiation and photo probe – which locates at the top of the spherical bomb (i.e., near the end of the vertical tube) – it can be known whether a successful detonation is first initiated in the vertical tube. Using the TOA measurement from the piezoelectric shock pin located at the bottom of the spherical chamber, it is then possible to distinguish between successful detonation transmission and failure. For example, successful transmission and failure cases in a stoichiometric C_2H_2/O_2 mixture with the tube diameter of 19.1 mm and initial pressures of p_o = 12 kPa and 11 kPa are shown in Fig. 2.3 and 2.4, respectively. It can be seen from Fig. 2.3 that at an initial pressure of 12 kPa, the arrival time of the expanding wave is 201 μs when it reaches the photo probe and 317 μs at the shock pin. The computed velocities of the wave are 2073.4 m/s and 2136.7 m/s in the vertical tube and spherical chamber, which are 91.1% and 94.4% of the CJ detonation velocity, respectively. It shows that at an initial pressure of 12

kPa, the tube diameter is above the critical value, thus the planar detonation can successfully transit into a spherical detonation. While for an unsuccessful transmission, Fig. 2.4 shows that when the initial pressure decreases to 11 kPa, although a detonation wave propagates in the vertical tube at a velocity around 90% CJ detonation velocity, the detonation fails after exiting into the free space and the velocity of the expanding wave is only 23.6% of the CJ velocity value. Hence, the measurement of traveling time of waves from ignition to the arrival time to the shock pin is sufficient to determine 'go/no go' due to the time scale difference between arrival times for high-speed deflagration and detonation being very different.

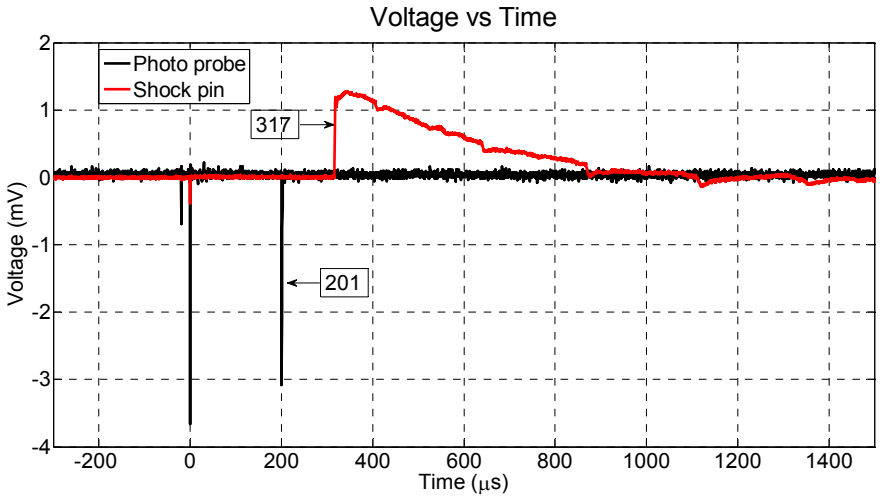

Figure 2.3 Arrival time trace of a planar detonation emerging into an unconfined space: successful initiation of a spherical detonation in stoichiometric $C_2H_2 + 2.5O_2$ mixture at an initial pressure of 12 kPa.

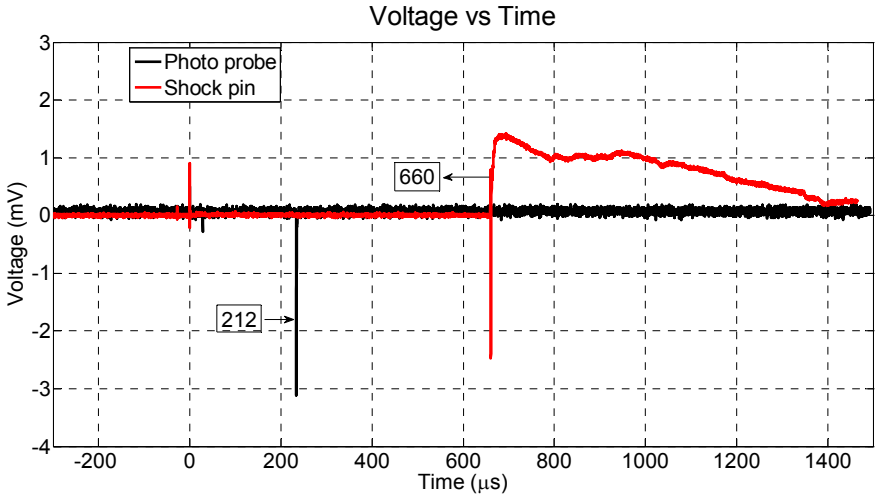

Figure 2.4 Arrival time trace of a planar detonation emerging into an unconfined space: unsuccessful initiation of a spherical detonation in stoichiometric $C_2H_2 + 2.5O_2$ mixture at an initial pressure of 11 kPa.

To ensure statistical convergence and reproducibility of the results, each experiment with same conditions (i.e., mixture composition, initial pressure p_o, and tube diameter D) was repeated eight times in order to identify accurately the critical pressure value above which a spherical detonation can form at each tube diameter. The sensitivity of the mixtures was varied by the initial pressure. The critical condition for each mixture is characterized by the critical pressure below which the detonation fails to emerge into the large spherical chamber. Figure 2.5 shows a sample result showing the test matrix and all go/no go data, i.e., successful and unsuccessful transmission of the detonation wave from the confined circular tube to the open area in the spherical chamber. Due to the inherent experimental variability, in the present analysis, the critical pressure is defined by the upper limit boundary above which at least 75% of tests at the same initial condition give a successful transmission of the detonation wave into the open space. All the data fluctuations are thus below this upper limit and a relative change between different cases can still be revealed. This criterion provides a meaningful way for relative comparison due to the difficulty in obtaining an extensive set of data to carry out a statistical analysis.

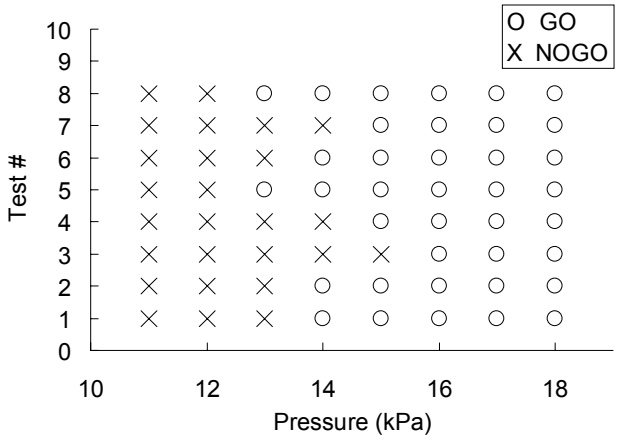

Figure 2.5 A sample set of go/no go result for an experiment.

2.3 Sources of Measurement Errors

To provide a degree of accuracy of the results, this section summarizes all the possible source of uncertainties in different measurement and how these affect the outcome of the present investigation. For the length scale measurement such as the diameter of the tube, a conservative estimate of its uncertainty is given to be ± 0.1 mm (The digital Vernier Caliper has an accuracy of ± 0.01 – 0.02 mm). The pressure transducer used to monitor the pressure has a range of 0 – 30

psi with an accuracy of ± 0.25 % full scale and this is equivalent to about 0.52 kPa. The digit meter is calibrated to display the minimum pressure reading of 0.01 kPa. Taking all the above into consideration, the pressure measurement is estimated to have a degree of confidence at least ± 1 kPa. It should be mentioned that in subsequent Chapters one assumes the cell size correlation provides reasonable estimate and did not consider in the present study the statistical error for the scaling analysis. This requires a detailed analysis of different cell size measurement from various sources and this is beyond the scope of this thesis work.

2.4 Validation and Comparison with Published Data

To check the reliability of the present experimental facility, direct measurement of the critical tube diameter are carried out in a number of common combustible mixtures (i.e., C_2H_2+O_2, C_2H_2+2.5O_2, C_2H_2+4O_2, C_2H_4+3O_2, C_3H_8+5O_2, C_2H_2+2.5O_2+50%Ar, C_2H_2+2.5O_2+70%Ar) by Zhang et al. (2013a). The critical tube diameter for various mixtures as a function of initial pressure obtained by experiment is shown in Fig. 2.6. Other correlations for undiluted mixtures, which are based on the experimental data measured by Matsui and Lee (1978), are also included for comparison, represented by the solid lines in the plots. It can be seen from Fig. 2.6 that for the undiluted mixtures, the experimental data from this study is in good agreement with those found in Matsui and Lee (1978).

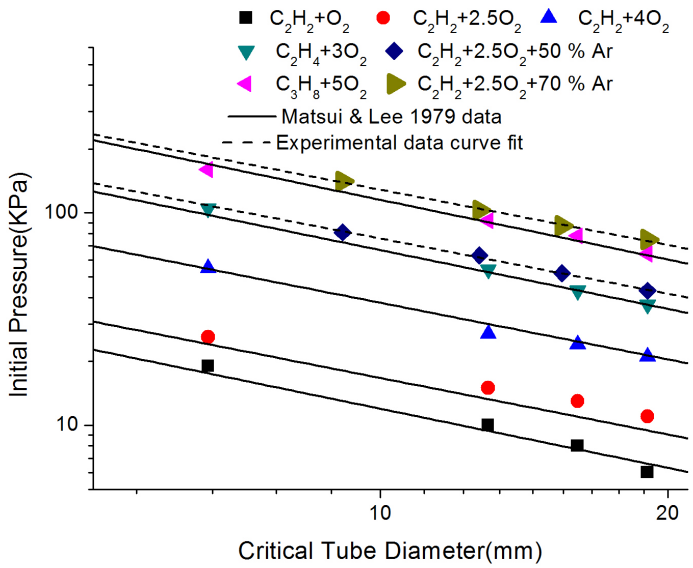

Figure 2.6 Comparison of the critical tube diameter measurement with those by Matsui and Lee (1978).

Following previous studies, it is worth to correlate the present critical tube diameter results with available detonation cell size data tabulated in CALTECH Detonation Database (Kaneshige and Shepherd 1997). The curve fit correlations of available cell size data as a function of initial pressure for the mixtures considered in this study are given in Table 2.1. By comparing the critical tube diameter and cell size as shown in Fig. 2.7, it is found for the undiluted mixtures (i.e., C_2H_2-O_2, C_2H_2-2.5O_2, C_2H_2-4O_2, C_2H_4-3O_2, C_3H_8-5O_2) the relationship between these two parameters is $d_c \approx 13\lambda$. This observation is in good agreement with previous investigations (Mitrofanov and Soloukhin 1965; Knystautas et al. 1982). Similar to previous results obtained by many researchers (Desbordes et al. 1993; Moen et al. 1986; Sherpherd et al. 1986), the present experiment data also confirms that for mixtures highly diluted with argon, the $d_c \approx 13\lambda$ correlation breaks down. It is found that the proportional factor equals 21 and 29 for the stoichiometric acetylene-oxygen mixtures with 50% and 70% argon dilution, respectively. Detonations in highly argon diluted mixtures are stable and their propagation mechanism is different from that of cellular detonations in unstable mixtures (Radulescu 2003; Lee 1996), thus the failure and re-initiation of a diffracting stable detonation emerging from a tube into unconfined space are also different, resulting in the breakdown of $d_c \approx 13\lambda$. This issue will be studied in more detail in Chapter 3.

Mixtures	***C***	**α**
C_2H_2-O_2	9.2382	0.9625
C_2H_2-2.5O_2	26.262	1.1889
C_2H_2-4O_2	54.967	1.1656
C_2H_4-3O_2	56.458	0.9736
C_3H_8-5O_2	186.55	1.1729
C_2H_2-2.5O_2-50%Ar*	61.5	1.12
C_2H_2-2.5O_2-70%Ar*	113.8	1.20

** From Radulescu (2003)*

Table 2.1 Cell size correlations as a function of initial pressure given by**:** λ [mm] = $C\cdot(p_o$ [kPa]$)^{-\alpha}$

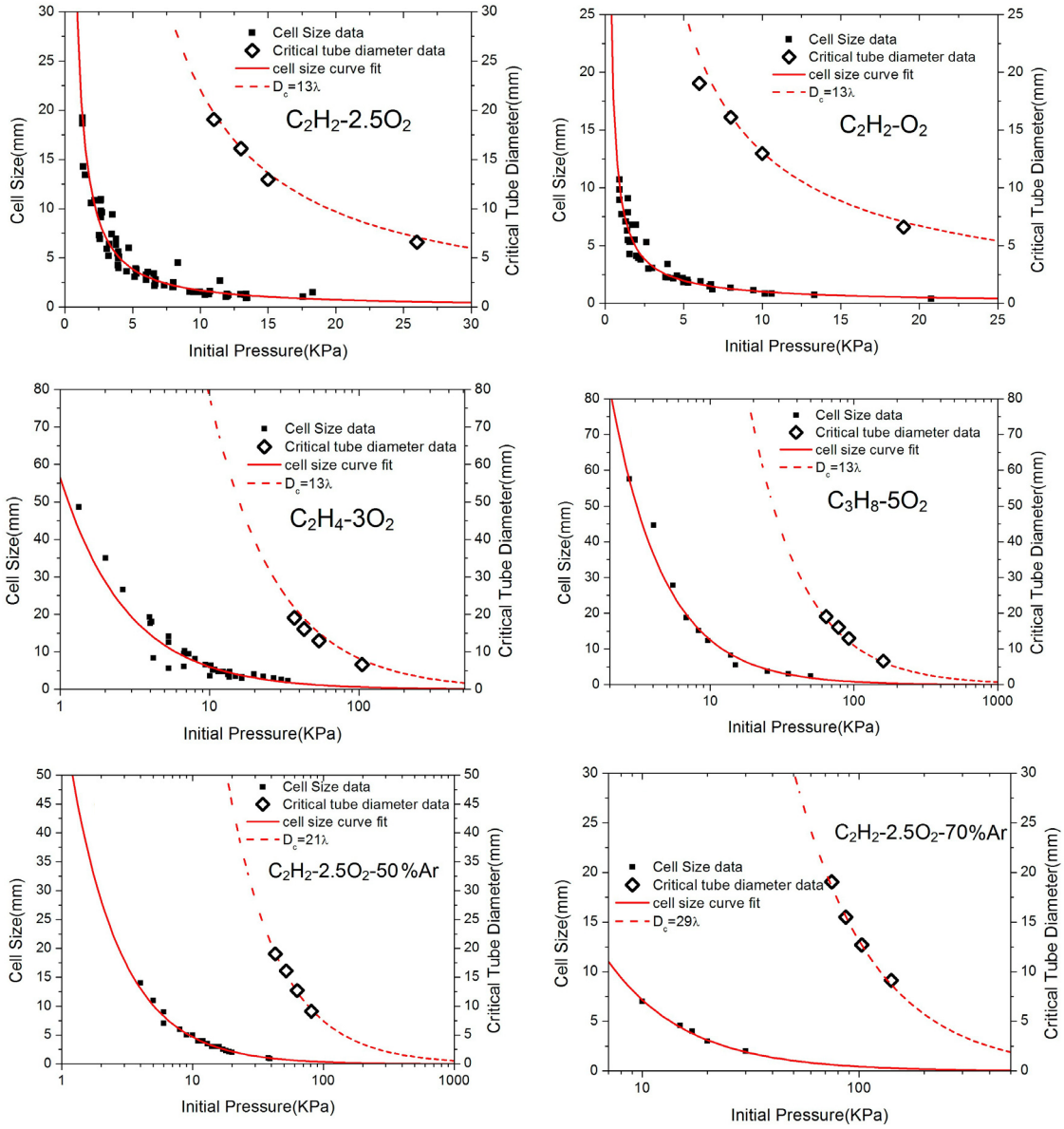

Figure 2.7 Critical tube diameter and cell size as a function of initial pressure for a) C_2H_2-2.5O_2; b) C_2H_2-O_2; c) C_2H_4-3O_2; d) C_3H_8-5O_2; e) C_2H_2-2.5O_2-50%Ar; and f) C_2H_2-2.5O_2-70%Ar mixtures (Zhang e al. 2013a).

2.5 Summary

In this Chapter, the general description of the experimental facility is provided. Measurement of the critical tube diameter is included for a number of hydrocarbon-oxygen mixtures and good agreement is shown between the present results with those published in the literature. The universal scaling of critical tube diameter with detonation cell size in this study and its breakdown also confirm the results reported in the previous literature.

Chapter 3

The Effect of Instability on the Critical Tube Diameter Phenomenon

In this Chapter, measurement of the critical tube diameter for stoichiometric acetylene-oxygen mixtures diluted with varying amount of argon is presented. By diluting with different amount of argon, the degree of detonation stability of the mixture can be modified and studied. The experimental results show that the critical tube diameter increases with the increase of argon dilution. The scaling behavior between the critical tube diameter d_c and the detonation cell size λ is systematically studied with the effect of argon dilution. The present results confirm that the relation $d_c \approx 13\lambda$ holds for 0% - 30% argon diluted mixtures and breaks down when argon dilution increases up to 40%. This critical argon dilution is close to that found from experiments in porous-walled tubes by Radulescu and Lee (2002) which exhibit a distinct transition in the failure mechanism. Cell size analysis in literature also indicates that the cellular detonation front starts to become more regular (or stable) when the argon dilution reaches more than 40 - 50%. The present experimental results thus agree qualitatively all the observations in the literature.

3.1 General Overview

As discussed in the thesis introduction, gaseous detonations in most hydrocarbon mixtures are generally unstable with an ensemble of transverse waves interacting at the shock front that forms the characteristic irregular cellular structure (Lee 2008). Using the detonation cell size λ to characterize the unstable cellular structure, dynamic parameters in these common mixtures usually follow well with classical empirical correlations. In a large wealth of literature on the diffraction of a planar detonation wave as it emerges from a circular tube into unconfined space, it was found that the critical tube diameter for many common hydrocarbon fuels-oxygen or -air mixtures is universally about 13 detonation cell widths of the mixture (i.e., $d_c \approx 13\lambda$) (Mitrofanov and Soloukhin 1965; Knystautas et al. 1982). Exceptions to these universal correlations were mixtures with high argon dilution (Sherpherd 1986; Desbordes et al. 1993; Moen et al. 1986). In these special cases of so-called highly "regular" mixtures with argon dilution, the critical conditions can vary as much as $d_c \sim 20$ to 30λ. The common explanation of the breakdown of 13λ rule is suggested to result from the unstable nature or difference in regularity between the detonation fronts in undiluted (unstable) and diluted (stable) mixtures. As shown in Chapter 1 that for undiluted hydrocarbon mixtures, typically with high activation energy in the chemical reaction (thus high reaction sensitivity), the cellular detonation front is unstable embedded with small scale instabilities and its propagation relies on the interactions of transverse waves (Shepherd 2009; Radulescu 2003). On the other hand, for detonations in combustible mixtures that have been highly diluted with argon, the detonation front is very regular or appears to be piece-wise laminar where cellular instabilities do not seem to play a prominent role on the propagation of a stable detonation (Radulescu et al. 2002).

To understand why argon has a stabilized effect on the regularity of the cellular detonation, Radulescu et al. (2002) carried a detailed study looking at the reaction zone structure with the effect of argon. From a chemical kinetic point of view, argon is a third body and participates only in the termination reaction. Thermodynamically, it does not influence the induction zone due to the increase in the specific heat ratio which compensates the decrease in energy content of the mixture by inert dilution. However, by diluted the mixture with large amount of argon, it is found that the heat release zone is much longer and smoother than the undiluted mixture, as shown in Fig. 3.1. The increase, with argon dilution, of the characteristic reaction zone length

during which the exothermic recombination processes occur can be explained by considering the changes in the elementary rates occurring at the end of the chain-branching steps and during the recombination steps of the oxidation scheme. As argon is added, the total heat release (per mole) decreases significantly, resulting in a lower temperature rise in the reaction zone. As a consequence of a lower temperature in the reaction zone, the chemical reaction rates of the exothermic reactions are reduced, leading to an increase in the heat release times. In other word, with a less steep profile the reaction rate is less temperature sensitive in highly argon diluted mixtures and the flow perturbation has less effects and growth rates. Referring to the cartoon shown in Fig. 3.2, the energy release is more "coherent" and continuous. With less sensitive to any flow perturbation generating high degree of instability in highly argon diluted mixtures, this makes the structure more ideal and approaches to the ideal ZND description.

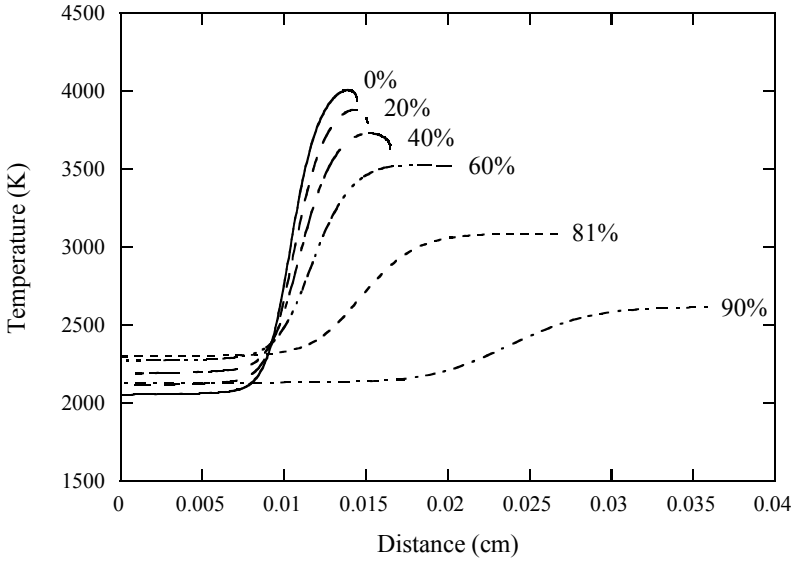

Figure 3.1 Steady ZND temperature profiles for stoichiometric acetylene-oxygen detonations with different degrees of argon dilution (Radulescu et al. 2002).

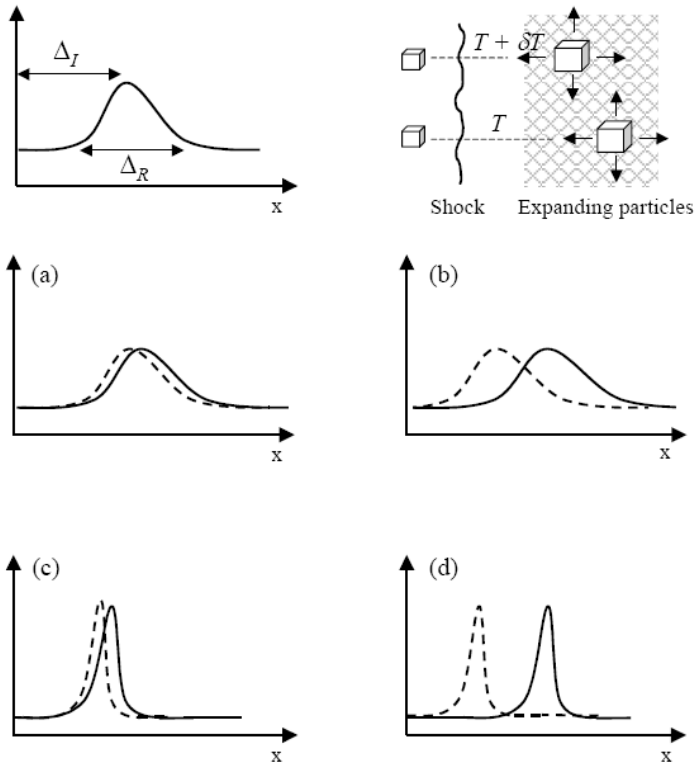

Figure 3.2 An illustration of the coherence concept between neighboring power pulses, given by the exothermicity profiles for two neighboring gas elements shocked at temperatures differing by δT. (a) Small temperature sensitivity, long exothermic reaction length; (c) small temperature sensitivity, short exothermic reaction length; and (d) large temperature sensitivity, short exothermic reaction length. Only case (d) results in incoherence of power pulses and the development of instability (Radulescu 2003; Ng and Zhang 2012).

As such, highly-argon diluted mixtures were often considered as special mixtures to investigate the effect of instability on the dynamics of detonation initiation and propagation, failure in detonation limits and the critical tube diameter problem (e.g., Radulescu and Lee 2002; Desbordes et al. 1993; Radulescu et al. 2002; Chao et al. 2009; Zhang et al. 2011a). Since in highly argon diluted mixtures, the propagation is believed to rely mainly on the shock ignition mechanism (Radulescu 2003) and the instability should not play a major role. As discussed in Chapter 1, detonation limits in tubes and the transmission of a detonation wave from a confined tube into a sudden open area are also thought to be governed by a global failure mechanism (Lee 1996). This mechanism appears to be driven from excessive front curvature, above a critical value of which a steady ZND detonation can no longer be obtained (Camargo et al. 2010; Klein

et al. 1995; Yao and Stewart 1995). Evidences also pointed out that the local instability seems not to play a prominent role in the critical tube diameter problem (Lee 1996).

To demonstrate the deviation from the universal scaling and elucidate the origin of the two possible modes of propagation and failure mechanism, i.e., one caused by suppression of instability and the other by excessive curvature, previous studies often considered the two extreme cases, i.e., detonations in undiluted C_2H_2-O_2 mixtures and diluted C_2H_2-O_2 mixtures with heavy amount of argon addition more than 70%. In the literature, no study systematically investigates the quantitative effect of increasing amount of argon dilution on the behavior of the detonation wave and its critical tube diameter. It is of interest not only to look at the transition of the two proposed distinct modes of propagation and failure mechanism, but also to study different scaling relationships and to determine what quantity of argon diluent in the explosive mixture such that cellular instabilities start to become less significant in the detonation dynamics. In this Chapter, the critical tube diameter in stoichiometric acetylene-oxygen mixtures diluted with varying amount of argon from 0% to 70% at different initial pressures are measured experimentally. New experimental data of critical tube diameter are reported, and the relation between the cell size and critical tube diameter along with increasing amount of argon dilution in stoichiometric acetylene-oxygen mixtures is then discussed.

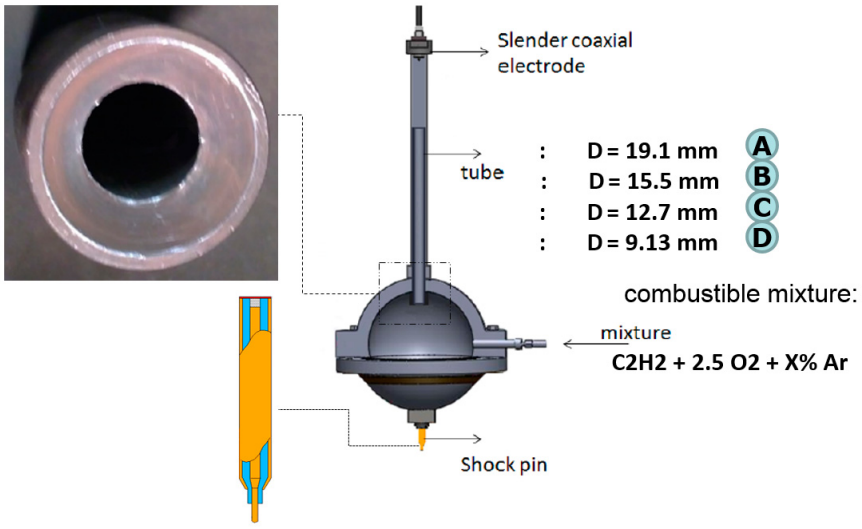

Figure 3.3 Schematic of the critical tube diameter experiment.

3.2 Experimental Details

The experimental facility used for the present experiment is described previously in Chapter 2 and a similar schematic of the apparatus is shown in Fig. 3.3. All four diameters of the vertical tube D were considered, i.e., D = 19.1, 15.5, 12.7 and 9.13 mm. Mixtures of stoichiometric C_2H_2–O_2 with different argon dilutions from 22% to 70% were investigated. The explosive mixture was prepared beforehand in separate vessel by the common method of partial pressure. The sensitivity of the mixtures was controlled by the initial pressure p_o and the range is given in Table 3.1. All the procedure including the method to determine the critical condition from the measurement follows the description given in Chapter 2 and details are omitted here.

Ar,%	**p_o(kPa)**
0	11-21
22	13-27
30	16-33
40	25-51
50	43-81
65	55-99
70	75-141

Table 3.1 Initial conditions used in the critical tube diameter experiment.

3.3 Results and Discussion

Figure 3.4 first shows the experimental results and curve fits of critical tube diameter as a function of critical pressure for varying degree of argon dilution from 0% to 70% in stoichiometric acetylene–oxygen mixtures. The critical initial pressure is measured and is defined as the condition below which the emergent planar detonation from the vertical steel tube fails to transmit into large spherical chamber. It can be seen from Fig. 3.4 that the critical

pressure increases consequently with increasing amount of argon dilution at the same tube diameter. Equivalently, this result indicates that the detonation is less sensitive with larger amount argon dilution. As one can deduce intuitively, the critical pressure value is also shown to be lower when a circular tube with larger diameter D is used for the same mixture.

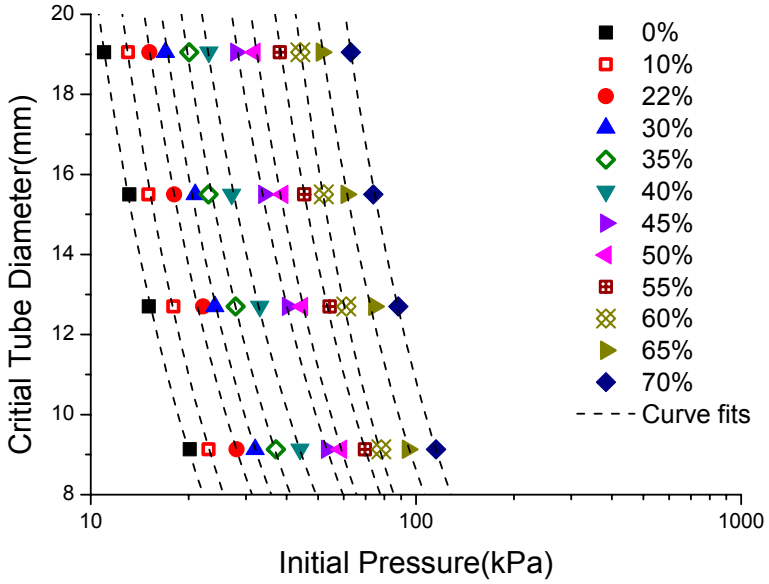

Figure 3.4 Variation of the critical tube diameter with initial pressure for different amount of argon dilution in stoichiometric $C_2H_2 + 2.5O_2 +$ %Ar mixtures.

Ar, %	C	μ
0	28.7	1.26
22	39.6	1.21
50	61.5	1.12
65	93.1	1.20
70	113.8	1.20
75	152.0	1.15
81	367	1.23

Table 3.2 The cell size correlation for $C_2H_2 + 2.5O_2 +$ %Ar mixtures as a function of initial pressure given by: λ [mm] $= C\cdot(p_o$ [kPa]$)^{-\mu}$ (parameters taken from Kaneshige and Shepherd 1997; Radulescu 2003).

From the present results of the critical tube diameter for direct initiation of detonations in $C_2H_2 + 2.5O_2 + \%Ar$ mixtures, it is shown that the effect of increasing argon dilution leads to higher values of this dynamic detonation parameter. In other words, high argon diluted acetylene–oxygen detonations are more susceptible to failure and harder to initiate. To further analyze the present experiment data, it is of interest to investigate the scaling between the cell size λ and critical tube diameter d_c in mixtures diluted with different amounts of argon. Part of the required cell size data for $C_2H_2 + 2.5O_2 + \%Ar$ mixtures can be found in CALTECH detonation database (Kaneshige and Shepherd 1997) and in the Radulescu's dissertation (2003). Unfortunately, the cell size data for mixtures with 30% and 40% argon dilution are not available and therefore, those values are estimated by interpolation from the available data of other argon dilution percentage. The cell size correlations as a function of initial pressure for different amounts of Argon dilution are reproduced in Table 3.2, and the corresponding plot is shown in Fig. 3.5.

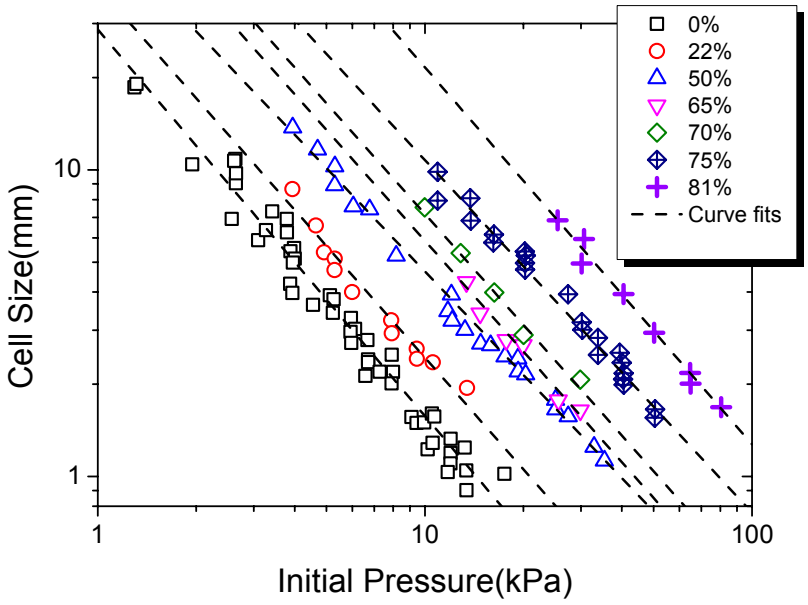

Figure 3.5 Cell size as a function of initial pressure in $C_2H_2 + 2.5O_2 + \%Ar$ (Kaneshige and Shepherd 1997; Radulescu 2003).

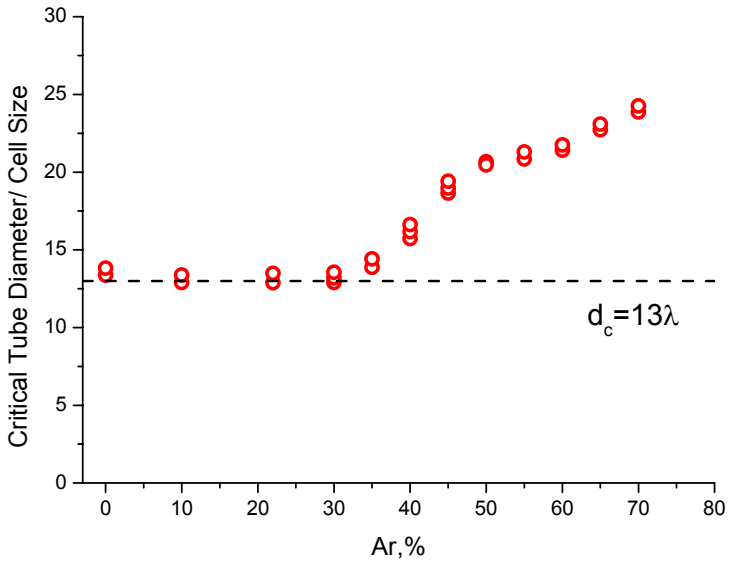

Figure 3.6 Critical tube diameter as a function of cell size for varying amount of argon dilution in stoichiometric $C_2H_2 + 2.5O_2 + \%Ar$ mixtures.

Figure 3.6 illustrates the behavior between the critical tube diameter and the cell size in $C_2H_2 + 2.5O_2$ mixtures diluted with argon varied from 0% to 70%. For stoichiometric acetylene–oxygen mixtures without and with small argon dilution (i.e., 0% and 22%), the critical tube diameter is found to be closely about 13 times the detonation cell size λ. Taken into account the uncertainty of cell size values, this indeed agrees reasonably well with the classical empirical correlation of $d_c \approx 13\lambda$. The correlation $d_c \approx 13\lambda$ still holds for mixtures with argon dilution of 30%. When the argon dilution reaches 40%, the proportionality factor between critical tube diameter and cell size gradually increases. Argon dilution up to 65% and 70%, exhibit factor increases close to 25, which is in good agreement with the results from Desbordes et al. (1993). As shown in Fig. 3.6, this transitional behavior in d_c/λ appears to be rather abrupt when the argon dilution reaches about 40–50%.

The breakdown of $d_c \approx 13\lambda$ relationship in mixtures when argon dilution is above 40–50% suggests that there is a transition in the detonation dynamics. Indeed, this critical amount of argon dilution agrees approximately with experiments in porous tubes where evidences show that there is also a distinctive change in the failure mechanism near approximately 50–60% argon dilution (Radulescu & Lee 2002; Radulescu 2003). This critical argon dilution corresponds roughly to the limit between regular and irregular cell structures, where highly regular cells were

observed above the same degree of argon dilution (Vandermeiren and Van Tiggelen 1984; Shepherd et al. 1986). Studies suggest that below this amount of argon dilution, the cellular detonation front remains highly unstable and the cellular instabilities play a dominant role in the self-sustained propagation (Radulescu 2003; Radulescu et al. 2002; Ng et al. 2005). For explosive mixtures with argon dilution more than 50%, the detonation becomes stable and regular in the sense that the role of cellular instabilities are less prominent in the propagation mechanism of stable detonations in these mixtures.

3.4 Summary

In this investigation, critical tube diameter was measured for stoichiometric acetylene–oxygen mixtures diluted with varying amount of argon. It is shown that the critical tube diameter increases with the increase of argon dilution. The effect of argon dilution on the scaling between different dynamic detonation parameters was then investigated. By comparing the critical tube diameter with the available cell size data in literature, it is found that the classical $d_c \approx 13\lambda$ relationship holds for 0–30% argon diluted mixtures; while increasing the amount of argon, the proportionality factor approaches 25 with 70% argon dilution. The change appears to be abrupt and the transition is thought to be due to dynamic effects in the detonation behavior, i.e., the detonation remains unstable and cellular instabilities play a dominant role in the self-sustained propagation of the detonation in mixtures without or with small amount of argon dilution. For cases with increasing argon dilution (e.g., above 40–50%) the detonation structure becomes regular and its propagation subsequently relies on the classical ZND shock ignition mechanism. The results of the present experiment thus clearly demonstrate the dependence between the detonation instability and the critical tube diameter.

Chapter 4

The Effect of Finite Perturbations on the Critical Tube Diameter Phenomenon

In this Chapter, an experimental investigation is carried out to further study the critical tube diameter problem for the transmission of gaseous detonation from a confined tube into a sudden open space in both regular mixtures, those highly diluted with argon and irregular mixtures of which the cellular detonation is highly unstable. The two commonly postulated modes of failure consisting of one by a local failure mechanism that is linked to the effect of instabilities for undiluted mixtures, and the other due to the excessive curvature of the global front in mixtures highly diluted with argon, are further investigated through experiments. To discern between these mechanisms in the different mixtures, flow perturbations are imposed by placing a minute obstacle with small blockage ratio at the tube exit diameter just before the detonation diffraction. Results show that the perturbation only has an effect in undiluted mixtures resulting in the decrease of the critical pressure for successful detonation transmission. In other words, the flow

fluctuation caused by the small obstacle produces transmission and this result seems to indicate that local hydrodynamic instabilities are significant for the detonation diffraction in undiluted unstable mixtures. On the other hand, the results appear to be the same for both unperturbed and perturbed cases in highly argon diluted mixtures. The small blockage only produces flow fluctuations and does not substantially influence the global curvature of the emergent detonation wave as illustrated in the numerical gasdynamic simulation and hence, it shall not affect the failure mechanism of the stable detonation in highly argon diluted mixtures. The observed phenomenon is also shown to be geometry independence of the obstacle even for the irregular mixtures of which the cellular detonation is highly unstable. This means that as the blockage ratio for a specific tube is kept constant, regardless of its blockage configuration the imposed perturbation shows almost an identical behavior for the wave transmission in irregular mixtures while has no major effect on this detonation dynamic parameter in regular ones.

4.1 General Overview

As discussed in the previous chapter, for common hydrocarbon mixtures, the critical tube diameter can be scaled universally through the characteristic cell size of the detonation front with $d_c \approx 13\lambda$. Nevertheless, results have shown that this empirical relationship breaks down for mixtures that are highly diluted with argon or for mixtures of which the detonation front is highly regular. This effect appears to result from the unstable nature or difference in regularity between the detonation fronts in undiluted (unstable) and diluted (stable) mixtures. The scope of the study presented in this Chapter is to design new critical tube diameter experiments that could unambiguously discriminate between the two postulated modes of failure and the link between the regularity of the instability pattern on the detonation front and the critical tube diameter introduced in the Chapter 1 and 3.

Present experiments are carried out in three different combustible mixtures, i.e., stoichiometric mixtures of undiluted acetylene-nitrous oxide, acetylene-oxygen as well as acetylene-oxygen with 70% of argon dilution, that range from highly irregular (unstable) to regular (stable) mixtures. While explicitly analyzing the gaseous detonation front and visualizing the detonation diffraction process may be challenging, an alternative way to study the detonation structure and to illustrate distinctly the different failure mechanism is to perturb the detonation

before the divergence and verify how the phenomenon responds. Hence, small flow perturbations are created purposely by a slender obstacle with minimal blockage ratio to ensure that significant large scale disturbances are not created, and also to minimize shock focusing downstream of the obstacle. In addition, several blockage configuration of the obstacle on the wave transmission in mentioned mixtures will also be investigated. The goal is to study the effect of hydrodynamic fluctuations and the significance of these localized instabilities at the detonation fronts in irregular (undiluted) or regular (argon diluted) combustible mixtures, as well as their effect on the successful transmission or failure of the detonation propagation from a confined tube into an abrupt area enlargement.

4.2 Experimental Details

The critical tube diameter experiments are conducted in the same detonation facility described in Chapter 2, see the schematic of the apparatus given in Fig. 4.1. In addition, in this experiment, a number of reactive mixtures including stoichiometric mixtures of acetylene-nitrous oxide, acetylene-oxygen, and acetylene-oxygen with 70% argon dilution are tested in this experimental study. These mixtures were also prepared beforehand in separate gas bottles by the common method of partial pressure. Same methodology using the TOA signal from the shock pin as described in Chapter 2 is used to determine the critical condition for each mixture is characterized by the critical pressure below which the detonation fails to emerge into the large spherical chamber.

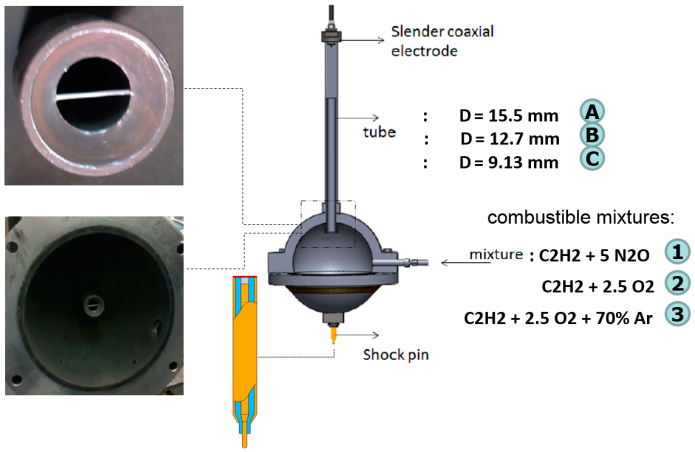

Figure 4.1 Schematic of the critical tube diameter experiment with perturbation.

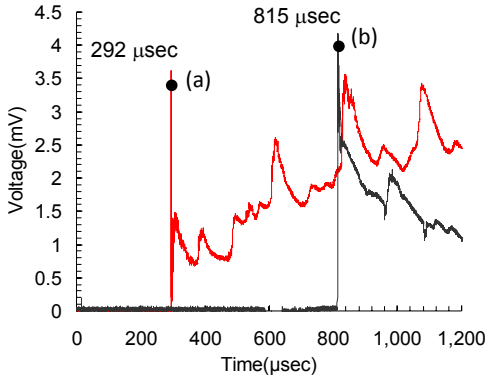

Figure 4.2 Signal from shock pin measurement.

For example, typical traces for a surviving emergent detonation wave from the tube to the open space and a detonation failure case in a stoichiometric C_2H_2–O_2 mixture with the tube diameter of 15.5 mm and initial pressures of p_o = 15 and 11 kPa are illustrated in Fig. 4.2. It can be seen from Fig. 4.2(a) that at an initial pressure of 15 kPa, the arrival time of the expanding wave is 292 μs when it reaches the shock pin. From the time between ignition and arrival at the shock pin, the wave velocity is determined to be approximately 2127 m/s, which is roughly 93% of the CJ detonation velocity. This illustrates that at an initial pressure of 15 kPa, the tube diameter is above the critical value, and thus the planar detonation can successfully transit into a spherical detonation. On the other hand, when the initial pressure is decreased to 11 kPa, an unsuccessful transmission ensues as shown in Fig. 4.2(b). Here, the expanding wave reaches the piezoelectric pin only at 815 μs. Hence, the detonation fails after exiting into the free space and the velocity of the expanding wave is roughly 33% of the CJ velocity value.

To investigate the effect of small perturbations on the critical tube diameter phenomenon, a flow disturbance was generated by the insertion of a slender needle at the exit diameter of the vertical tube, see Fig. 4.1. Three different sizes of needles were inserted for the three different tube diameters in order to keep the blockage ratio constant; i.e., using the biggest needle of diameter 1.0 mm for the large size tube (D = 15.5 mm), the needle of diameter 0.8 mm for the midsize tube (D = 12.7 mm) and the needle of diameter 0.6 mm for the small-size tube (D = 9.13 mm). The blockage ratio is kept approximately equal to 0.08.

It is worth noting that for the mixtures chosen in this investigation, dilution with argon changes the stability of the cellular detonation and makes the reaction rate less temperature sensitive or the detonation more stable (Ng and Zhang 2012). Although the dilution effect of

argon lowers the energetic of the mixture, on the other hand it also causes an increase in the specific heat ratio, resulting in an increase of the post-shock temperature. Therefore, there should be no substantial weakening in diluted mixtures at critical conditions for detonation transmission of each mixture and the magnitude of the gasdynamic effect of the obstacle is comparable. In this study, the effect of the obstacle is always compared relative to perturbed and unperturbed cases for the same mixture.

4.3 Results and Discussion

In this study, three kinds of gas mixtures were considered, i.e., stoichiometric C_2H_2-N_2O, C_2H_2-O_2, and C_2H_2-O_2 diluted with 70% of argon. These three mixtures qualitatively represent the cases for highly irregular (highly unstable), unstable and stable (highly regular) cellular detonation structures, respectively. Experimental observation on the regularity of the cell size pattern, made it possible to compute the stability parameter for each mixture as a figure of merit which serves to characterize the sensitivity of the mixtures (Radulescu 2003; Ng et al. 2005), and it is given by:

$$\chi = \varepsilon_I \frac{\Delta_I}{\Delta_R} = \varepsilon_I \Delta_I \frac{\dot{\sigma}_{\max}}{u'_{CJ}} \tag{4.1}$$

where ε_I is the effective normalized activation energy in the induction zone, Δ_I the induction length, and Δ_R the reaction length approximated by the inverse of the maximum thermicity ($1/\dot{\sigma}_{\max}$) multiplied by the CJ particle velocity u'_{CJ} in shock-fixed coordinates with the thermicity given by:

$$\dot{\sigma} = \sum_{i=1}^{N_s} \left(\frac{W}{W_i} - \frac{h_i}{C_p T} \right) \frac{dY_i}{dt} \tag{4.2}$$

where W denotes the mean molar mass of the mixture, C_p the mixture specific heat at constant pressure, and y_i, h_i the mass fraction and the specific enthalpy of specie i, respectively. The effective activation energy in the induction process ε_I can be obtained by constant-volume explosion calculations (Ng et al. 2005). Chemkin package (Kee et al. 1989) and the San Diego

chemical reaction mechanism were used to compute different chemical kinetics properties including the activation energy and various chemical length scale. The San Diego reaction mechanism has been validated and optimization targets of this mechanism included the detonation of acetylene-oxygen-diluent systems (Varatharajan and Williams 2001). Figure 4.3 compares relatively the stability parameter as a function of initial pressure for the three mixtures considered in this study. As the results shown, C_2H_2-N_2O is the most unstable mixtures among the three with the relatively largest value of χ and the argon dilution to the C_2H_2-O_2 mixture decreases its stability parameter making the mixture more stable. As discussed in Radulescu et al. (2002) and Ng et al. (2005), the variation in this stability parameter can be linked to the regularity of the instability pattern on the detonation front. In other words, both C_2H_2-N_2O and undiluted C_2H_2-O_2 are described by an irregular cellular structure while 70% Ar-diluted C_2H_2-O_2 is characterized by a very regular cellular structure, in accordance to experimental observations of smoke foil measurement, see Shepherd et al. (1986); Radulescu (2003); Ng and Zhang (2012) or Fig. 4.4. Therefore, Echoing the hypothesis by Lee (1996) on the critical tube diameter problem, the mechanism of detonation failure should be different in C_2H_2-N_2O and undiluted C_2H_2-O_2 mixtures with irregular cellular detonation structure, to that with diluted C_2H_2-O_2 with regular ZND-like detonation structure where instabilities is found to not playing a dominant role.

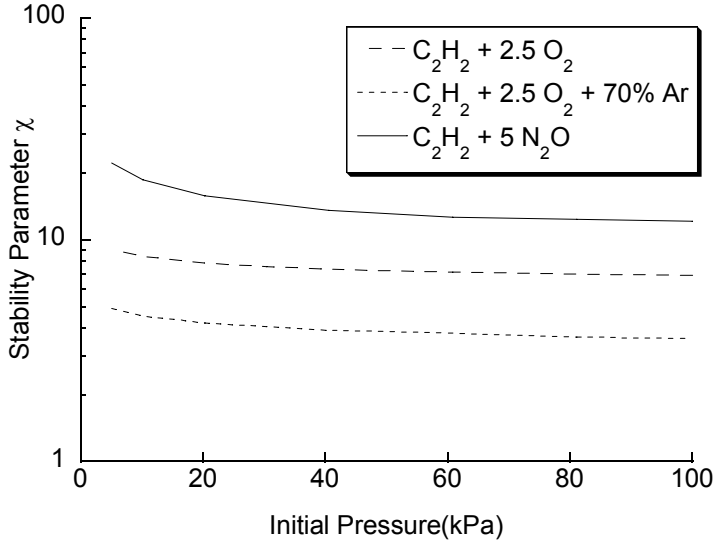

Figure 4.3 Stability parameter χ as a function of the initial pressure p_o for stoichiometric C_2H_2-N_2O, C_2H_2-O_2, and 70% Ar-diluted C_2H_2-O_2 combustible mixtures.

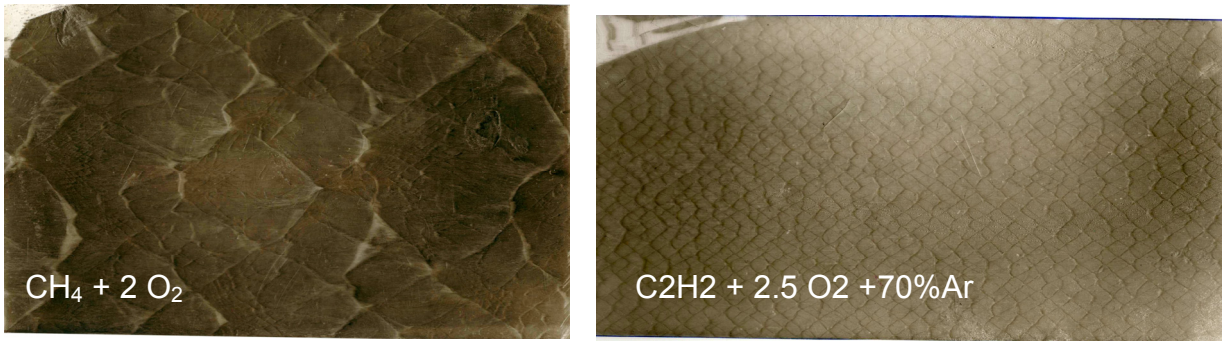

Figure 4.4 Smoked foil measurement.

Using all the obtained data in the present investigation, summary of all go/no go results is plotted in Fig. 4.5. Figure 4.5a) first shows the results for the C_2H_2-N_2O mixture and the critical pressure limits with and without perturbation for all three tube diameters D. For this mixture, it can readily be seen that the perturbation has an influence on the critical tube diameter phenomenon by lowering the critical pressure values for the successful transmission. The reduction in critical pressure caused from the perturbation for the three tubes are 2, 4 and 12 kPa, respectively for D = 15.5, 12.7 and 9.13 mm (or equivalently about 3.0, 4.8 and 9.8% difference where % difference is defined by [100% – (x/y · 100%)] where x and y are the lower and higher number). Similar behaviors are observed for the undiluted stoichiometric C_2H_2-O_2 mixture, shown in Fig. 4.5b). The difference in critical pressure between the perturbed and unperturbed cases are respectively 2, 3 and 6 kPa (or equivalently about 18.2, 18.8 and 28.6% difference) for the three tube diameters D = 15.5, 12.7 and 9.13 mm. From the results of both undiluted irregular mixtures, it appears that the effect of perturbation by the small needle is more apparent for the smallest size tube (i.e., D = 9.13 mm) used in this study. Despite the fact that the blockage ratio is kept the same for all three tube diameter experiments, the location of the needle (and the three-dimensional effects) could perhaps play a role on the results. Although the amount of disturbance was not quantitatively measured in this study, its trend suggests an agreement for all three scales D and the flow perturbation induced by the needle appears to promote transmission resulting in the decrease in critical pressure. Another observation from the results is that although C_2H_2-N_2O is more unstable compared to C_2H_2-O_2, the effect of the perturbation by the needle seems to be more significant for the latter mixture. Some explanation can perhaps be made within the scope of the spontaneous flame concept, originally proposed by Zel'dovich (1980). According to this

concept, the origin of explosion center and the mechanism leading to the onset of detonation is conditioned by the gradients of self-ignition time delay in the reactive fluid. Later studies also show that in order for any hydrodynamic fluctuation to grow or eventually initiate a detonation, the disturbance must be sufficiently strong and the critical size must be long on the order of the reaction scale to induce a gradient of thermal ignition time (Short 1997; Kapila et al. 2002; Lee et al. 1978). The later condition leads to the coupling between the propagation and amplification of the disturbance with the chemical energy release in the reactive medium (Lee et al. 1978). Table 4.1 shows the relative comparison between the size of the perturbation, roughly estimated by the integral scale of the needle diameter d_{needle}, to the chemical induction length scale of the two unstable mixtures Δ_I at the critical pressures for the normal case without perturbation. As shown in the table, the ratio $(d_{needle}/\Delta_I)_{critical}$ for the C_2H_2-O_2 mixture is bigger than the C_2H_2 + 5 N_2O mixture for all three tube diameters D and the biggest tubes in both cases have smaller ratios. The bigger value of the ratio $(d_{needle}/\Delta_I)_{critical}$ for the C_2H_2-O_2 mixture therefore suggests that the perturbation is large enough and has turbulent strength, consequently it can reside longer on the order of the chemical induction time and is more effective to promote a spontaneous explosion center that supports the transmission of the detonation into the unconfined area.

Mixture	D **(mm)**	d_{needle} **(mm)**	$p_{critical}$ **(kPa)**	Δ_I **(mm)**	$(d_{needle}/\Delta_I)_{critical}$
C_2H_2 + 5 N_2O	15.5	1.0	67	8.74×10^{-2}	11.4
	12.7	0.8	85	6.77×10^{-2}	11.8
	9.13	0.6	124	4.62×10^{-2}	13.0
C_2H_2 + 2.5 O_2	15.5	1.0	14	5.23×10^{-2}	19.1
	12.7	0.8	16	4.40×10^{-2}	18.2
	9.13	0.6	21	3.22×10^{-2}	18.6

Table 4.1 Comparison of the ZND induction length with the size of the perturbation at critical conditions. The induction length Δ_I is computed using the San Diego chemical mechanism.

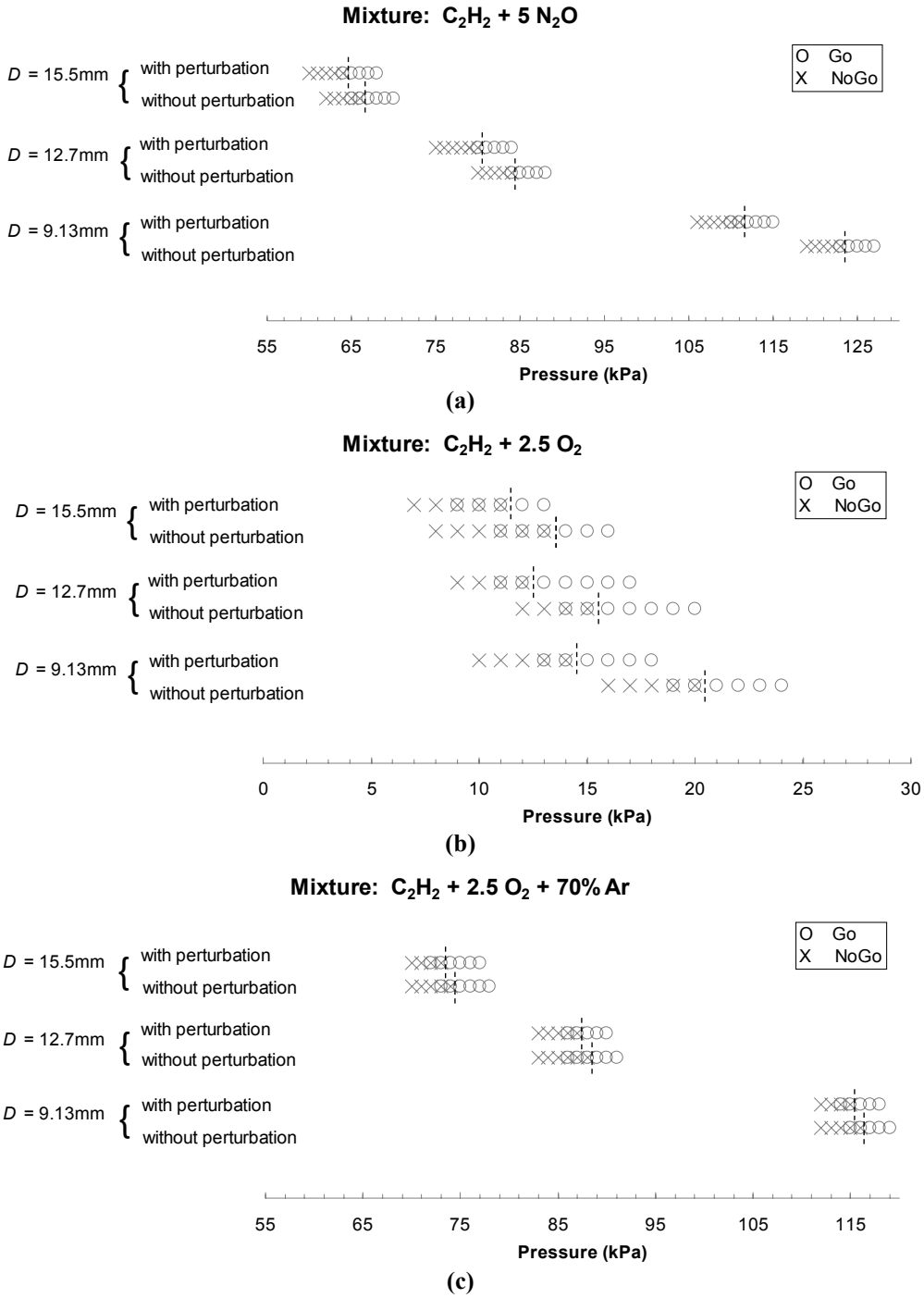

Figure 4.5. Summary of go/no go results for all three combustible mixtures with/without the presence of the needle to create perturbation.

On the other hand, the results of Fig. 4.5c) show that the transmission of detonation from the unconfined tube to the open area in the C_2H_2-O_2 mixture highly diluted with argon appears not to be affected by the perturbation. The difference in critical pressure between the perturbed and unperturbed cases in all three tube diameters is less than 1 kPa or approximately 1%. Taking into

account the experimental uncertainty which includes the metering panel for the initial filled pressure measurement, it can be concluded that for this argon diluted mixture, essentially the same critical pressure limits between successful and unsuccessful transmission of diverging detonations in the open space are obtained for all tube diameters. Therefore, these results demonstrate that the critical condition for successful detonation transmission is not very sensitive to the flow perturbation by needle.

For the undiluted mixtures where the reaction kinetics is sensitive to flow disturbances and the detonation propagation or transmission relies on the instabilities at the front, i.e., role of the transverse waves, the additional flow perturbations created by the needle compensate the instability suppressed/quenched by the failure wave for the case without perturbation and re-generate local explosion center for successful transmission. In contrast, for diluted mixtures of which the detonation front is very regular or stable and the role of instability does not play a prominent role, the failure mechanism is dominantly caused by the global curvature and as the numerical results in the following qualitatively show, the needle with minimal blockage ratio and the flow disturbance induced does not affect significantly the wave front curvature.

To illustrate qualitatively the effect of the minute needle on the gasdynamic flow field in the experiment, numerical simulation using a simplified two-dimensional geometry was conducted. It is important to emphasize that the numerical simulation is not intended to reproduce the full reactive flow phenomenon of detonation diffraction, which is computationally expensive and often under-resolved. The purpose of the present simple but reliable inert shock simulation is to illustrate qualitatively that the obstacle does not have a global effect of the leading diffracted wave curvature, hence it does not influence the failure mechanism of the diffracted detonation in diluted mixture. Approximating the solutions of Euler equations by the 2^{nd} order Roe's flux difference splitting (FDS) scheme with spatial resolution of 0.06 mm and CFL number of 0.5 using the software ANSYS-FLUENT, it was possible to simulate a Mach M = 6 shock diffraction in air (γ = 1.4) with the interaction of a cylinder at the exit of the channel. Although this represents only a two-dimension simulation, the physical dimensions were kept as close to those used in the experiments. The small channel and the opening chamber has a width of 9 mm and 25 mm, respectively and the cylindrical obstacle has a diameter of 0.6 mm. To illustrate the gasdynamic change caused by the small obstacle, Fig. 4.6 shows the temperature contours from the numerical simulation. Without the pin obstacle, the wave diffracts and the expansion waves

continues to enter the center core and reduces the flow temperature behind the wave front, see Fig. 4.6a). For perturbed case shown in Fig. 4.6b), upon the wave interaction with the small obstacle, a number of transverse waves disturbances are generated and regions (including the front) with localized temperature fluctuation can be seen. However, the global curvature of the diffracted wave does not change much. As explained earlier for unstable mixtures with high reaction sensitivity, these hydrodynamic fluctuations will have an effect on the detonation diffraction to promote local explosion centers for successful transmission. In contrast to regular mixtures where instabilities are not the dominant mechanism in transmission, once the leading front fails due to the excessive curvature from the diffraction, the perturbation will not be able to give rise to a transmitted detonation.

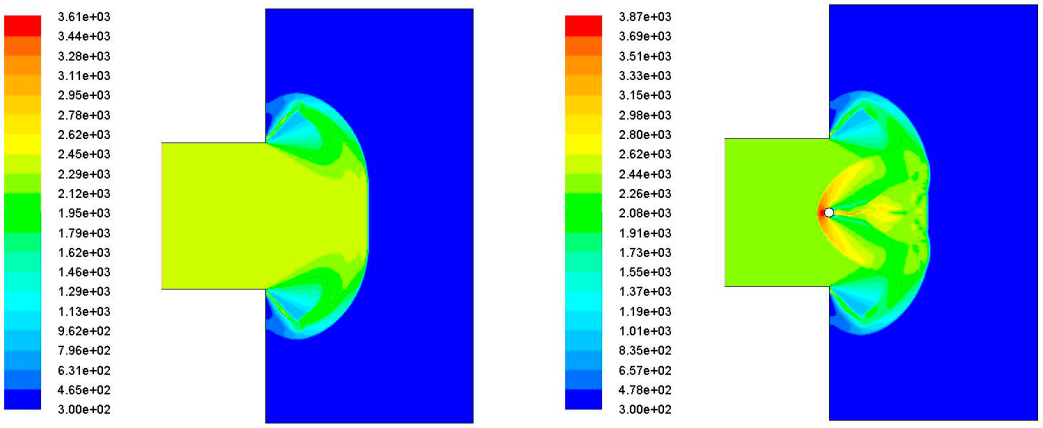

Figure 4.6. Temperature contour plots from the numerical simulation of the diffraction of a Mach 6 shock in air. a) unperturbed case; and b) perturbed case with a small pin obstacle.

Theoretically, it may perhaps be possible to explain the observation using an energy-drag approach, an analysis similar to detonation initiation by high speed projectile (Vasiljev 1994; Lee 1997; Verreault and Higgins 2011). Through the drag force, the small obstacle can deposit an amount of energy into the product flow mixture. The work done by the drag force of the needle of diameter d_c and length l (which is equal to the diameter of the detonation tube D) can be written as:

$$F_D = \frac{1}{2} C_D A_f \rho_{CJ} u_{CJ}^2 \qquad (4.3)$$

where F_D is the drag force, A_f is the frontal or projected area (here for a cylinder of length $L = D$, this area is equal $d_{needle}*D$), C_D the drag coefficient and ρ_{CJ}, u_{CJ} are the CJ density and particle

velocity of the detonation product flow, respectively. Because the free-stream cross-flow is of high Reynolds number, the drag coefficient of the cylindrical needle takes approximately on a number value of 1.0. Lee's work done model (1978) can then be used to estimate the energy deposition given by:

$$E_D = \int_0^{t^*} F_D u_{CJ} dt \tag{4.4}$$

where t^* is modeled as the time when the rarefaction wave reaches the tube axis, which can be approximated by $t^* \sim D/2a_{CJ}$ with a_{CJ} being the sound speed of the detonation products (Matsui and Lee 1978; Vasil'ev 1998). Hence, using the drag force,

$$E_D = \frac{C_D \rho_{CJ} u_{CJ}^3 d_{meedle} D^2}{4a_{CJ}} \tag{4.5}$$

It is of interest to compare this work done by drag to the critical energy required to initiate a spherical detonation in the unconfined space. Based on the work done model by Lee (Desbordes 1988; Sochet et al. 1999; Zhang et al. 2012b), it is assumed that the energy needed to re-initiate a detonation downstream of the unconfined space in the critical tube diameter problem can be related to the work done delivered by the detonation product in the confined tube (i.e., a fictitious piston) over the same period t^* given above, the energy can be obtained by:

$$E_s = \int_0^{t^*} p_{CJ} \frac{\pi d_c^2}{4} u_{CJ} dt \tag{4.6}$$

where p_{CJ} and u_{CJ} denote the CJ detonation pressure and particle velocity, respectively. After the integration the simplified work done model thus gives:

$$E_s = \frac{p_{CJ} u_{CJ} \pi d_c^3}{8a_{CJ}} \tag{4.7}$$

By comparing both energies E_D and E_s the following expression is obtained:

$$\frac{E_D}{E_s} = \frac{2C_D \rho_{CJ} u_{CJ}^2 d_{needle}}{\pi p_{CJ} D} \tag{4.8}$$

Based on this expression, Table 4.2 shows values of different parameters and compares the drag energy with the initiation energy at the critical condition for successful transmission in the unconfined area. The present estimation shows that the drag (energy) is at most ~ 3% (found to be roughly same for both diluted and undiluted mixtures) of that the mean detonation product

flow responsible for the initiation in the free space. This 3% is indeed negligible compared to the initiation energy change required for the observed decrease in critical pressures in undiluted mixtures. Such decrease in near critical pressure is equivalent to far more than 50% increase in initiation energy for a diverging detonation (Zhang et al. 2012a). Therefore, a global energy-drag approach is not a possible interpretation of physics for the present results. Although with the tiny obstacle some kinetic energy got converted to thermal one persisting downstream - resulted in local fluctuation or instability that can promote the transition in the undiluted mixtures but play no effect for less-temperature sensitive diluted mixtures with the failure due to the global curvature of the diverging wave only. These mechanisms are confirmed in this study by experiments and such confirmation represents the significant merit of this study.

Mixture	D **(mm)**	d_{needle} **(mm)**	p_{critical} **(kPa)**	p_{CJ} **(kPa)**	ρ_{CJ} **(kg/m^3)**	u_{CJ} **(m/s)**	E_D/E_S **(%)**
C_2H_2 + 2.5 O_2 + 70% Ar	15.5	1.0	75	1,727	2.023	810	3.26
	12.7	0.8	89	2,062	2.399	813	3.08
	9.13	0.6	117	2,740	3.152	817	3.21
C_2H_2 + 2.5 O_2	15.5	1.0	14	437	0.317	1,065	3.38
	12.7	0.8	16	502	0.362	1,068	3.30
	9.13	0.6	21	666	0.475	1,074	3.44
C_2H_2 + 5 N_2O	15.5	1.0	67	2,587	2.038	1,018	3.35
	12.7	0.8	85	3,310	2.585	1,022	3.27
	9.13	0.6	124	4,890	3.769	1,028	3.41

Table 4.2 Numerical values of different parameters and comparison between the drag energy with the initiation energy at the critical condition for detonation transmission

Experiments were also carried out with other perturbation geometries, i.e., different configurations of the needle obstacle while keeping the overall blockage ratio constant. It can be seen from Figs. 4.7 and 4.8 showing the results for two different tube diameters D = 15.5 and 9.13 mm that the perturbation effect is geometry independence of the obstacle. In other words, as the blockage ratio for a specific tube is kept constant, regardless of its geometry or needles configuration, results show almost identical behavior. For the irregular mixtures all the results

with different needle(s) perturbations show similar decrease in critical pressure for successful transmission. On the other hand, for the mixture highly diluted with argon, where it has been suggested that the cellular instabilities play minor roles in the detonation propagation mechanism, the flow perturbation (despite different arrangement) does not have any major effect on the phenomenon.

4.4 Summary

In this investigation, the critical tube diameter phenomenon and the failure mechanism for detonation diffraction in three combustible mixtures, ranging from highly irregular to regular detonation structures are studied. Gasdynamic disturbances were introduced using a needle with small blockage ratio at the exit of the tube before the gaseous detonation emerges into the free unconfined space. By observing how the detonation responds to the flow perturbation during the diffraction, it is possible to investigate the important role of instability and to provide confirmation on the two postulated mode of failure mechanism proposed by Lee (1996) on the phenomena of critical tube diameter.

For the cases of undiluted stoichiometric C_2H_2-N_2O and C_2H_2-O_2 mixtures in which the detonation wave is highly unstable and relies on the instability at the cellular front, it is found that the additional flow perturbation can cause a noticeable effect on the detonation diffraction. Despite a difference due to the scale effect, all the results of the three tube diameters with needle perturbations show a decrease in critical pressure for successful transmission. On the other hand, for the mixture highly diluted with argon – where it has been suggested that the cellular instabilities play minor roles in the detonation propagation mechanism, the flow perturbation does not have any major effect on the phenomenon. Numerical simulations show that the hydrodynamic disturbance induced by the needle provides flow fluctuation behind the wave but does not significantly change the curvature of the diffracted wave. This result appears to support a curvature based mechanism for failure in these stable mixtures rather than the suppression of instability by the failure wave and the inability to generate local explosion centers.

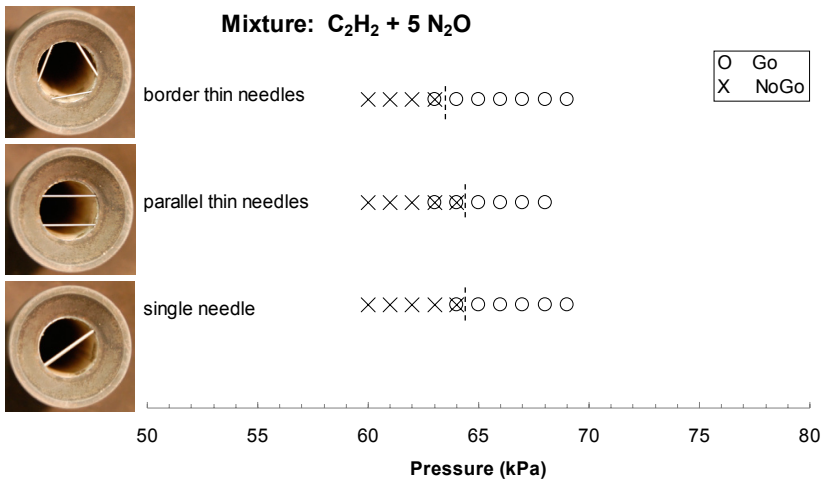

(a)

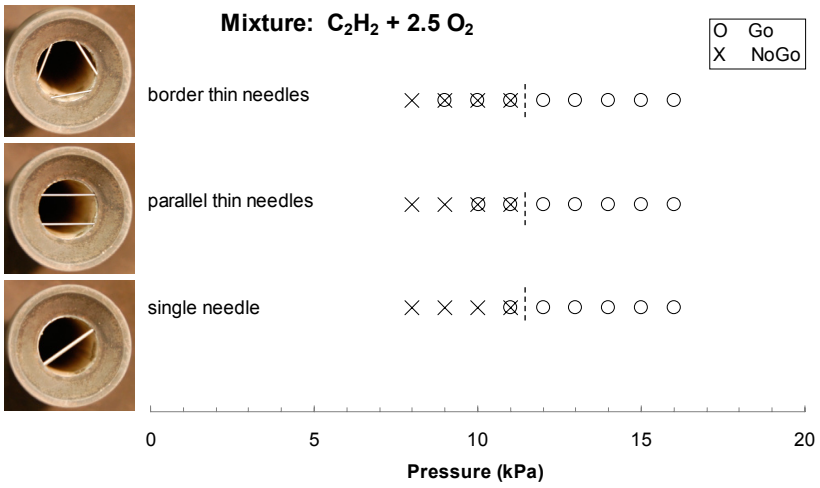

(b)

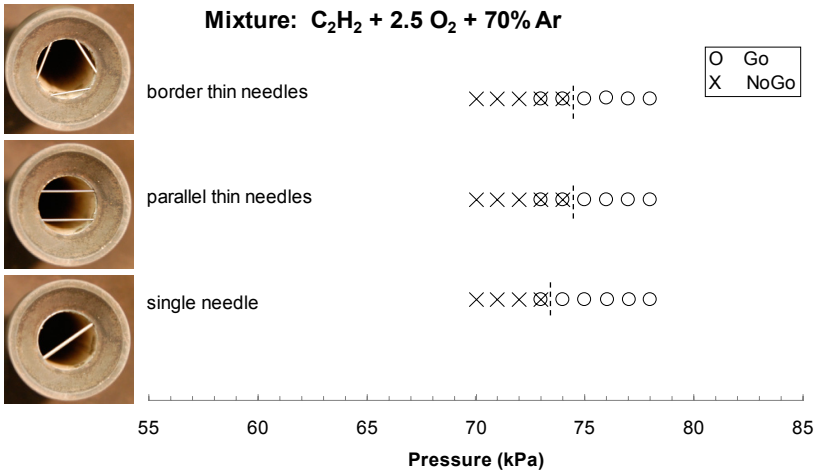

(c)

Figure 4.7 Summary of go/no go results for all three combustible mixtures with different needle arrangements (BR ~ 0.08) to create perturbation and tube diameter D = 15.5 mm.

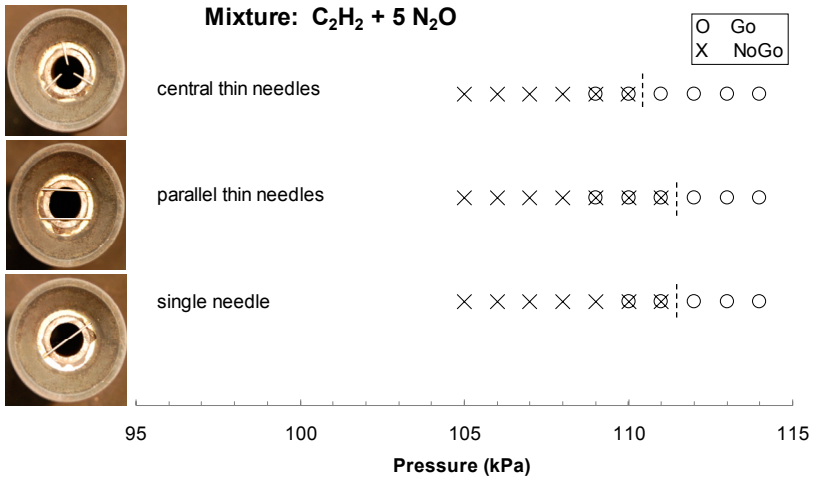

(a)

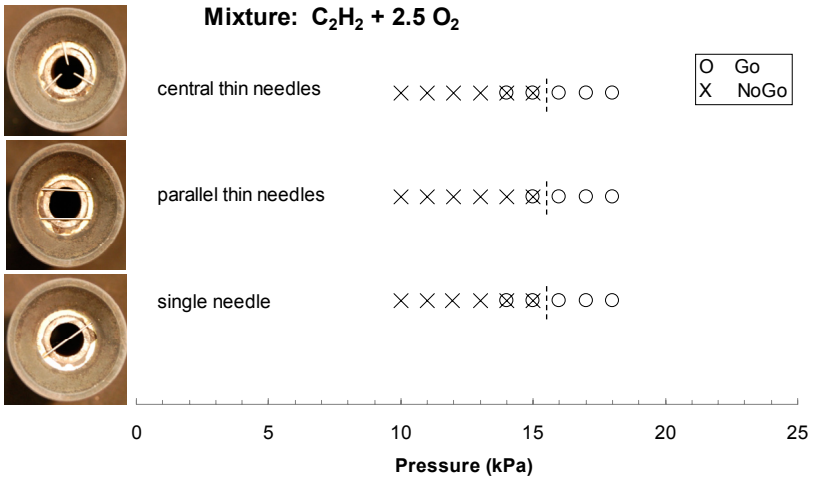

(b)

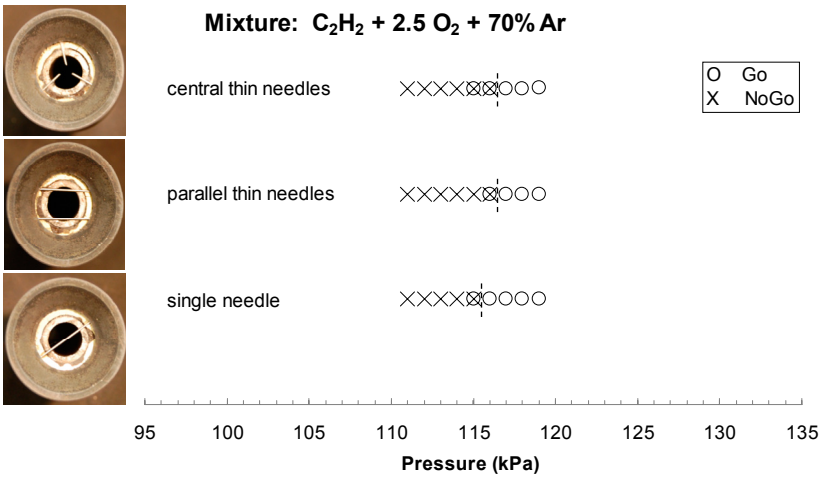

(c)

Figure 4.8 Summary of go/no go results for all three combustible mixtures with different needle arrangements (BR~ 0.08) to create perturbation and tube diameter D = 9.13 mm.

Chapter 5

A Technique for Promoting Detonation Transmission into Unconfined Space

A simple method for promoting detonation transmission from a small tube to a large area is presented. The idea stems from the result obtained in Chapter 4 using needle perturbation to facilitate the transmission of detonation from confined area into open space. More specifically, this technique involves placing obstacles which create slight blockages at the exit of the confined tube before the planar detonation emerges into the larger space, thereby generating flow instability to promote the detonation transmission. In this experimental study two mixtures of undiluted stoichiometric acetylene-oxygen and acetylene-nitrous oxide are examined. These mixtures can be characterized by a cellular detonation front that is irregular and representative of those potentially used in practical aerospace applications. The blockage ratio imposed by the obstacles is varied systematically to identify the optimal condition under which a significant reduction in critical pressure for transmission can be obtained. A new perturbation configuration

for practical use in propulsion and power systems is also introduced and results are in good agreement with those obtained using thin needles as the blockage ratio is kept constant.

5.1 General Overview

Recent focus on the development of detonation-based propulsion systems for high propulsive efficiency such as pulse detonation engines (PDE) (Nicholls et al. 1957; Eidelman 1992; Bussing and Pappas 1994; Kailasanath 2003; Lu 2009; Wang et al. 2013), has led to a renewed interest in the problem of detonation diffraction, i.e., detonation waves propagating from tubes of one size or geometry into another variable cross-section (Li and Kailasanath 2000; Fan and Lu 2008; Baklanov and Gvozdeva 1995), especially for the design of tube initiator geometries, e.g., when a detonation transmits from the small pre-detonator to the main thrust tube of the pulse detonation engine (Roy et al. 2004). For the successful and steady operation of the PDE, repetitive initiation of detonation waves is required. The pre-detonator tube diameter should be made above a critical value known as the critical tube diameter (Lee 1984), to ensure successful initiation in the larger detonation or thrust chamber tube and avoid detonation failure during diffraction. The objective of this work is to investigate the effect of hydrodynamic disturbance generated by small blockages on the detonation diffraction problem and propose a new practical design of the injector connecting the small tube section to a larger area, as it can have a beneficial effect for enhancing successful transmission of the detonation from different areas for PDE applications to aerospace propulsion and power systems.

Although no complete predictive theory has yet been developed, the criterion for successful transmission of a self-sustained detonation from a confined tube to an open area is often understood from the description of the failure mechanisms during detonation diffraction. Common hydrocarbon mixtures in which detonations are unstable with highly irregular cellular structures, successful transmission is often found to originate from a localized region in the failure wave, which is eventually amplified to sustain the detonation propagation front in the open area. Hence, failure is invariably linked to the suppression of instabilities at which localized explosion centers are unable to form in the failure wave when it has penetrated the charge axis (Lee 1996; Vasil'ev 2012).

The importance of instability for detonation transmission was demonstrated by the study given in Chapter 4. This study investigates the effect of finite perturbation generated by placing a small gauge needle that serves as an obstacle with a small blockage ratio (BR = 0.08 defined as the cross-sectional area of the needle divided by the inside cross-sectional area of the confined tube) at the tube exit diameter just before the detonation diffraction, and observing the phenomenon's response. For special mixtures such as highly diluted argon mixtures which are stable with regular cellular patterns, the results using this small needle perturbation seem to exhibit little variation in detonation pressure for both perturbed and unperturbed cases. This can be attributed to the minimal effect of the perturbations on global curvature for the emergent detonation wave. However, results show that the small perturbation can have a significant effect in undiluted hydrocarbon mixtures resulting in the decrease of the critical pressure for successful detonation transmission. In other words, the disturbance caused by the small obstacle promotes transmission and this result supports that local hydrodynamic instabilities are significant for detonation diffraction in typical undiluted unstable mixtures considered for detonation-based propulsion systems. Using different needle arrangements at the exit of the confined tube, the study presented in Chapter 4 also demonstrates that the perturbation effect is independent of the blockage geometry, and suggests that it is only a function of its imposed blockage area. In other words, as the blockage ratio is kept constant, regardless of its configuration, the resulting perturbations show an almost identical behavior for wave transmission in irregular mixtures whilst not affecting regular ones.

In the present study, the effect of disturbance on the critical tube diameter problem in undiluted stoichiometric acetylene-oxygen and acetylene-nitrous oxide mixtures are investigated. The originality of this work is to systematically observe the effect of different blockage ratios with BR varied from 0.05 – 0.25. It is worth noting that the tested mixtures have a detonation instability nature representative to those potentially used in experimental PDE such as hydrogen or ethylene-based mixtures. Intuitively, it is anticipated that large BR will have an adverse effect due to excess momentum losses caused by the blockage and reduction of the "effective" tube diameter. Therefore, this work attempts to determine the optimal value of which detonation transmission is favourably promoted. Another novelty of this work is to introduce a different practical perturbation arrangement designed in an attempt to further promote the detonation transmission for PDE application in aerospace propulsion and power generation.

5.2 Experimental Details

The experiments are carried out in the facility described in Chapter 2. Stoichiometric mixtures of acetylene-oxygen or acetylene-nitrous oxide are considered in this study. These were also prepared beforehand by the common method of partial pressure in separate gas bottles were tested. The mixture sensitivity is varied by changing the initial test pressures p_o. The procedure to run the experiment and to determine whether the emerging detonation from the confined tube is successfully transmitted into the open space using the time-of-arrival (TOA) measurement from the piezoelectric shock pin (CA-1136, Dynasen Inc.) located at the bottom of the spherical chamber are the same as described in Chapter 2. The critical condition for each mixture is again characterized by the critical pressure below which the detonation fails to emerge into the large spherical chamber.

To generate small perturbations and identify the optimal *BR* ratio using which detonation transmission can be promoted from a confined tube into larger space, slender needles of different sizes are inserted at the exit diameter of the vertical tube to vary the blockage ratio *BR* from 0.05 - 0.25. In the second part of the study, a novel perturbation configuration is designed as shown in Fig. 5.1 instead of using needles as the disturbance generator. The present "injector" is made out of steel cylindrical rod. The design takes into account the manufacturing challenge and durability of the obstacles. This design retains symmetry and for the D = 12.7 mm tube, three blockage ratios of this configuration were studied with BR = 0.095, 0.13 and 0.25. For the smaller tube diameter D = 9.13 mm, the injector with BR = 0.098 was built and tested.

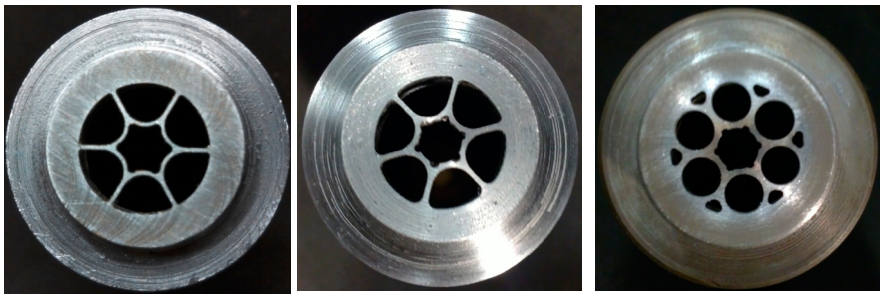

(i) (ii) (iii)

Figure 5.1 A new perturbation configuration with D = 12.7 mm. i) *BR* = 0.095; ii) 0.13; and iii) 0.25.

5.3 Results and Discussion

For each *BR* ratio considered, initial pressure was incrementally decreased until the critical value below which the detonation wave cannot successfully transmit from the confined circular tube to the open area in the spherical chamber is determined. An example of one set of experimental results is given in Fig. 5.2, showing the Go/No-go plot (or successful/unsuccessful transmission) as a function of initial pressure with *BR* = 8%. In these plots, the overlap between the two symbols indicates that there is a mixed result among the 8 experimental shots repeated at that particular initial pressure. Such occurrence near critical conditions can be due to inherent sources of experimental variability and is typical for any detonation experiment. In this study of critical tube diameter, the range of uncertainty is not as significant as compared to the measurement of critical energy for direct initiation and detonation cell size.

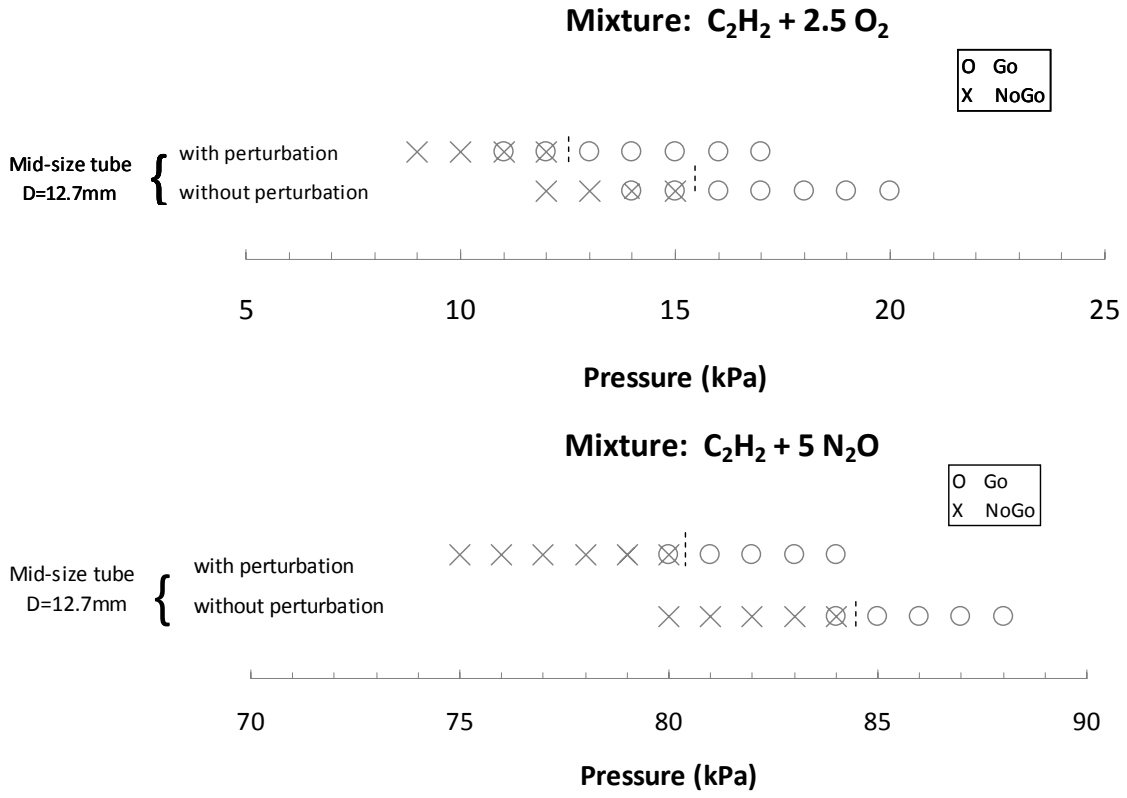

Figure 5.2 Sample Go/No-go plots as a function of initial pressure.

Figure 5.3 summarizes the measured critical pressure limits for the stoichiometric C_2H_2/O_2 and C_2H_2/N_2O mixtures with needle perturbation of each different tested blockage ratio *BR*. A blockage ratio of zero refers to the unperturbed case. Also shown in each plot is the curve fit obtained using least-square regression. From the results shown in Fig. 5.3, it is observed that for sufficiently small blockage ratios, the needle obstacles can have a noticeable influence on the critical tube diameter phenomenon by lowering the critical pressure values for successful transmission. The maximum reduction in critical pressure caused from the needle perturbation for both stoichiometric C_2H_2/O_2 and C_2H_2/N_2O mixtures are 3 and 4 kPa, respectively (or equivalently about 18.8% and 4.8% difference where % difference is defined by [100% – (x/y · 100%)] where x and y are the lower and higher number). It is observed that for both mixtures tested that the optimal reduction in critical pressure locates at approximately less than 10% blockage ratio. For very large *BR* (*BR* > 0.18), excess blockage leads to a negative effect, causing too much of a momentum loss, consequently the emerging detonation front will not promote the detonation transmission in the open space and actually increases the critical pressure dramatically.

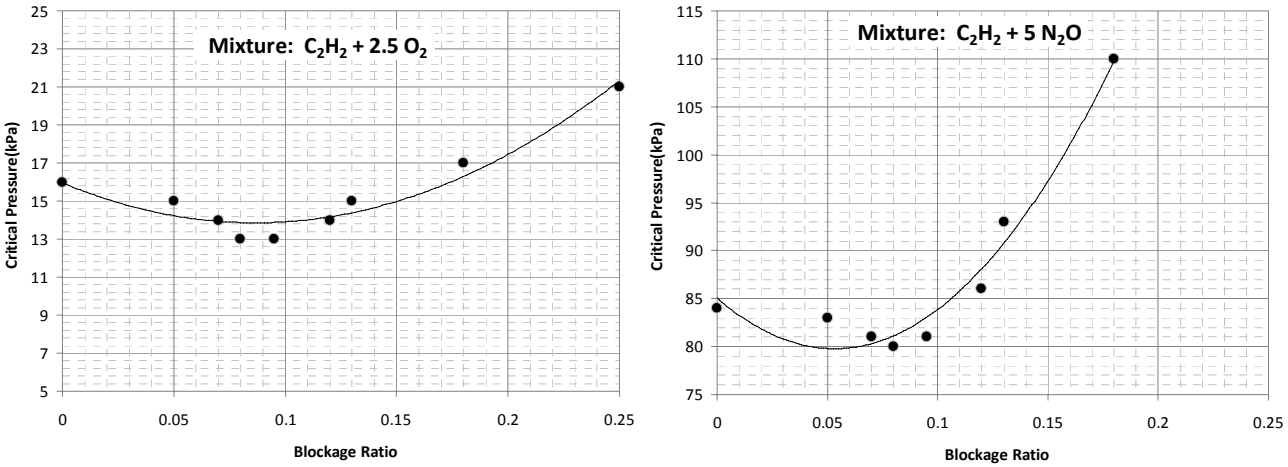

Figure 5.3 The effect of blockage ratio on the critical pressure for successful transmission.

An equivalent series of experiments are then performed using the new perturbation configuration. Figure 5.4 first presents the results for the large diameter tube D = 12.7 mm using the new "injector" configuration with BR = 0.095, 0.13 and 0.25. The plot shows the Go/No-go data and the critical pressure limits. Once again, for each experimental condition (i.e., mixture composition, initial pressure p_o and blockage ratio), the experiment was again performed 8 times to ensure repeatability of the results. It is found that these results are in good agreement with those previously obtained with needles, as is illustrated in Fig. 5.3. The optimal reduction in critical pressure for successful transmission occurs with the blockage ratio of 9.5% in both tested mixtures. Similarly, the maximum decreases in critical pressure between the perturbed and unperturbed cases are respectively 3 and 4 kPa for the stoichiometric C_2H_2/O_2 and C_2H_2/N_2O mixtures. The present result indeed confirms previous observations which postulate that while maintaining a constant blockage ratio, the effect is shown to be qualitatively independent of the obstacle geometry for the typical irregular hydrocarbon mixtures, whereby all the results with different needle(s) perturbations show similar decrease in critical pressure for successful transmission. Similarly as observed earlier, excess blockage to the flow (e.g., BR = 25%) results in an adverse effect, i.e., causing a significant increase in critical pressure required for detonation transmission.

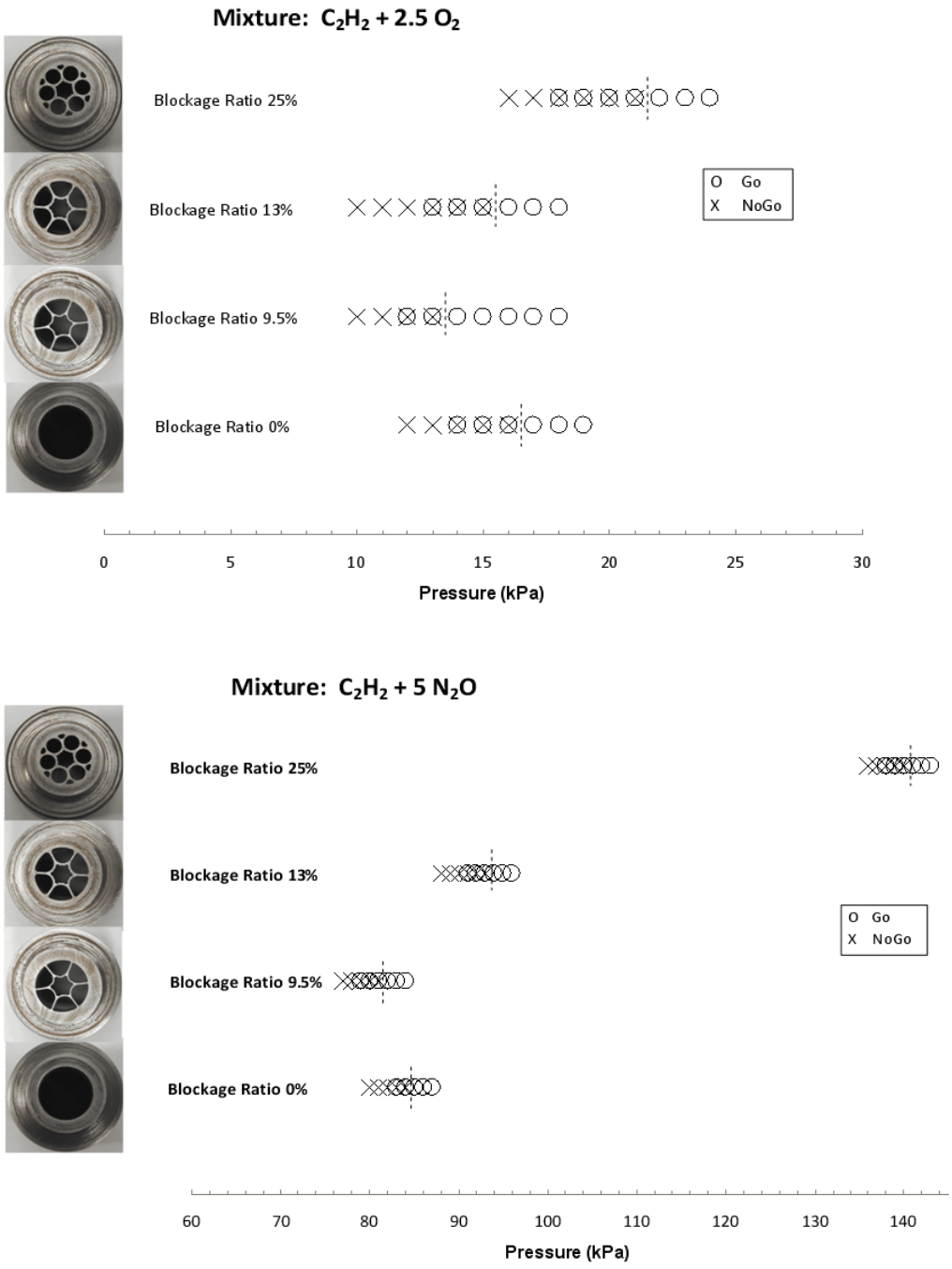

Figure 5.4 Summary of Go/No-go results for the two combustible mixtures with different BR of the injector and *D* = 12.7 mm.

The last set of experiments was performed for the smaller tube diameter D = 9.13 mm using the same type of injector configuration. The significant decrease in critical pressures can also be observed but more clearly for this smaller tube diameter with BR = 9.8% as shown in Fig. 5.5, with a maximum reduction of 6 and 12 kPa (equivalently a difference of 28.6% and 9.8%), respectively for the stoichiometric C_2H_2/O_2 and C_2H_2/N_2O mixtures.

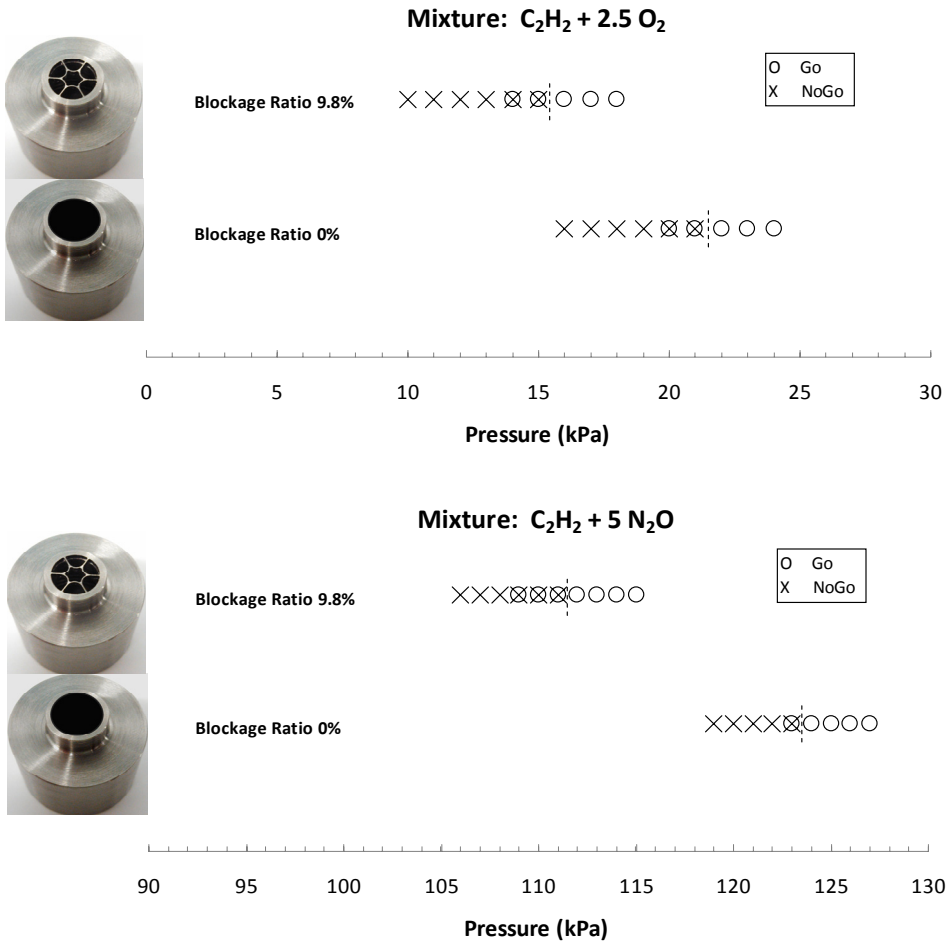

Figure 5.5 Summary of go/No-go results for the two combustible mixtures with BR = 9.8% and D = 9.13 mm.

5.4 Summary

In this study, the effect of small perturbations with varying blockage ratio on the critical tube diameter problem are investigated in two unstable mixtures, typically with irregular cellular pattern as found in most hydrocarbon mixtures. Perturbations were introduced using both needle insertion at the exit of the tube before the gaseous detonation emerged into the free unconfined space and as “injectors” machined from steel rod. In all cases, it is found that the optimal blockage ratio is approximately 8 to 10%. Furthermore, the results agree with previous studies that demonstrate the effects of maintaining a constant blockage ratio. Moreover, the effect is shown essentially to be independent of the obstacle (or perturbation) geometry for the irregular mixtures where all the results show similar decrease (or increase with excess blockage) in critical pressure for successful transmission. These results can provide useful insight for practical application to the design of pulse detonation engines for aerospace propulsion and power systems.

Chapter 6

Effects of Porous Walled Tubes on Detonation Transmission into Unconfined Space

Experiments were carried out to investigate the failure mechanisms in the critical tube diameter phenomenon for stable and unstable mixtures. It was previously postulated that in unstable mixtures where the detonation structure is highly irregular, the failure during the diffraction is caused by the suppression of the instability responsible for the generation of local explosion centers. In stable mixtures, typically with high argon dilution and where the detonation is characterized by very regular cell, the failure is driven by the excessive global front curvature above which a detonation cannot propagate. To discern these two failure mechanisms, porous wall tubes are used to attenuate the transverse instability before the detonation emerges into the unconfined space. Porous sections with length L/D from 0 to 3.0 are used with two confined tube diameters D = 12.7 and 15.5 mm. The present results show that when porous wall tubes are used, the critical pressure for unstable $C_2H_2 + 2.5O_2$ and $C_2H_2 + 5N_2O$ mixtures increases significantly. In contrast, for stable argon diluted $C_2H_2 + 2.5\ O_2 + 70\%$ mixtures, the results with porous wall

tubes exhibit little variation up to L/D = 2.5. For L/D > 2.5 a noticeable increase in critical pressure for argon diluted mixtures is also observed. This is dominantly caused by the slow mass divergence through the porous material inducing a curvature on the detonation front even before it emerges into the open area. The present experiment again demonstrates the importance of the transverse wave instability for typical hydrocarbon mixtures in critical situations such as the critical tube diameter experiment. For special cases such as highly argon diluted mixtures, the instability does not play a significant role in the failure and the propagation is controlled dominantly by the global curvature effect and the shock-ignition mechanism.

6.1. General Overview

This study continues to look at the problem of critical tube diameter, d_c, defined as the minimum diameter of a round tube for which a detonation emerging from it to an open space can continue to propagate. The experiment in this Chapter is again designed in the goal to discern the two modes of failure responsible for the critical tube diameter phenomenon suggested by Lee (1996): one is a local failure mechanism that is linked to the dynamics of instabilities in undiluted mixtures, while the other mechanism supposes failure is due to the excessive curvature of the global front, in stable mixtures highly diluted with argon. In Chapter 4 and 5, we investigates the effect of a finite perturbation generated by placing a small slender needle that serves as an obstacle with a small blockage ratio at the tube exit diameter just before the detonation diffraction and observing the phenomenon's response. In summary, it is found in these previous Chapters that the small perturbation can have an effect in undiluted hydrocarbon mixtures resulting in the decrease of the critical pressure for successful detonation transmission. In other words, the disturbance caused by the small obstacle promotes transmission and this result shows that local hydrodynamic instabilities are significant for detonation diffraction in typical, undiluted, unstable mixtures considered for detonation-based propulsion systems. For mixtures such as highly diluted argon mixtures, which are stable with regular cellular patterns, the results using this small needle perturbation do not show a significant difference between the perturbed and unperturbed cases. This is explained by the fact that the effect of the small perturbations on the global curvature for the emergent detonation wave is minimal.

This present study proposes another simple experiment to illustrate the effect of instability on the detonation transmission from a confined tube to an open space by investigating the suppression of perturbations rather than their generation. Unlike the experiment using slender obstacles to generate perturbations, it is possible to suppress "instabilities", i.e. "transverse waves", inside the confined tube before the detonation wave emerges into the open area. This can be done by using acoustically absorbent material, which has the ability to attenuate the transverse waves associated with cellular detonation fronts. Such a method using acoustic absorption was indeed employed by Dupré et al. (1988), Teodorczyk & Lee (1995) and more recently by Radulescu & Lee (2002) to demonstrate the essential role of transverse waves on the propagation of detonation waves in circular tubes or thin channels. In this work, we extend results from these earlier studies onto the critical tube diameter problem and consider the effect of absorbing walls placed at the exit of the confined tube before the detonation emerges into the open area. This experiment illustrates the effect of transverse waves on the detonation transmission, again confirms the two postulated failure mechanisms, and also contributes to practical applications such as in the design of detonation arrestors, a device to quench or stop detonation propagation from one confined region to another, larger space. While previous studies have sought to link the detonation cell size to the critical tube diameter, we concentrate here solely on the response of different mixtures, representative of regular and irregular mixtures, to changes in the porosity of the side wall in the critical tube diameter experiment. The detonation cell size is visualized only to ascertain that the chosen porous material has an effect on the transverse wave activity, but the magnitude of that effect is not quantified.

6.2 Experimental Details

Figure 6.1a shows the schematic of the experimental setup as described earlier in Chapter 2. For the present study, the exit of the vertical tube was made porous using ½" inner diameter soaker hose (Colorite SNUER12025 cut to fit the tube inner diameter) made of extruded rubber material. The length of the porous wall was varied from $L = 0$ to $3D$ where $L/D = 0$ means no porous material was inserted. The inner tube diameter was kept constant whether or not the porous insert was present as shown in Fig. 6.1b. The effect of the porous material mounted on

the wall was also tested in a detonation tube facility shown in Fig. 6.2. It consists of a steel driver section 65 mm in diameter and 1.3 m long. A polycarbonate test tube of various diameters was attached to the end of the driver tube and the porous material was mounted in the middle of the test tube. The smoked foil technique was used to reveal the attenuation effect of this porous wall section.

Stoichiometric mixtures of acetylene/nitrous oxide, acetylene/oxygen, and acetylene/oxygen with 70% argon dilution were tested in this experimental study. The first two mixtures exhibit irregular (unstable) cellular detonation structures, while the latter exhibits a stable detonation front with regular cellular patterns (Radulescu et al. 2002; Ng and Zhang 2012). Experimental details such as the procedure used to determine whether the emerging detonation from the confined tube was successfully transmitted into the open space is the same as described in Chapter 2.

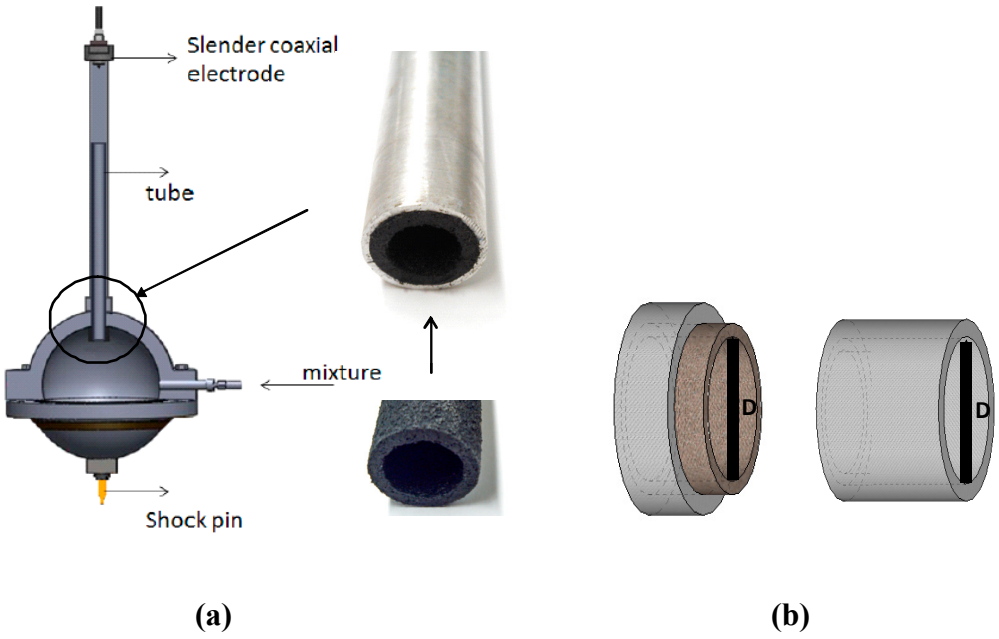

Figure 6.1 Schematic of a) the experimental facility; and b) porous walled tube.

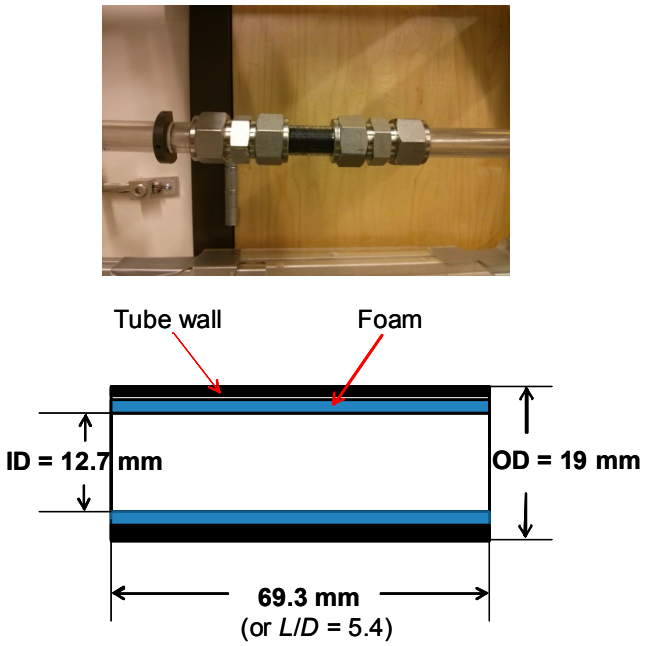

Figure 6.2 Porous walled region inside the test section of the detonation tube facility.

6.3. Results and Discussion

The smoked foil technique was used to look at the influence of the porous wall on the cellular detonation structure. As an example, Fig. 6.3 shows the smoked foils obtained for stoichiometric $C_2H_2 + 2.5O_2$ at different initial pressures. At an initial pressure sufficiently high for the detonation front to be multi-cellular, the smoked foils indicate, for all mixtures, a cell size increase and a subsequent return to the original cellular pattern after passage of the wave through the porous section. The effect of attenuation by the porous wall can be seen more clearly when the initial pressure is reduced. The damping by the porous media then causes the detonation wave to change from a multi-headed cellular front to a single headed spin downstream of the porous medium. Far away from the perturbation, the detonation re-establishes itself back to a multi-cellular front. For the case of p_o = 2 kPa, the incident detonation fails completely after passing through the porous wall section. Similar effects are observed for the stable mixtures with high argon dilution (i.e., stoichiometric $C_2H_2 + 2.5\ O_2 + 70\%$ Ar) as shown in Fig. 6.4. The results from this experiment thus indicate that the porous material used has the ability to damp out some transverse waves at the front for both stable and unstable mixtures.

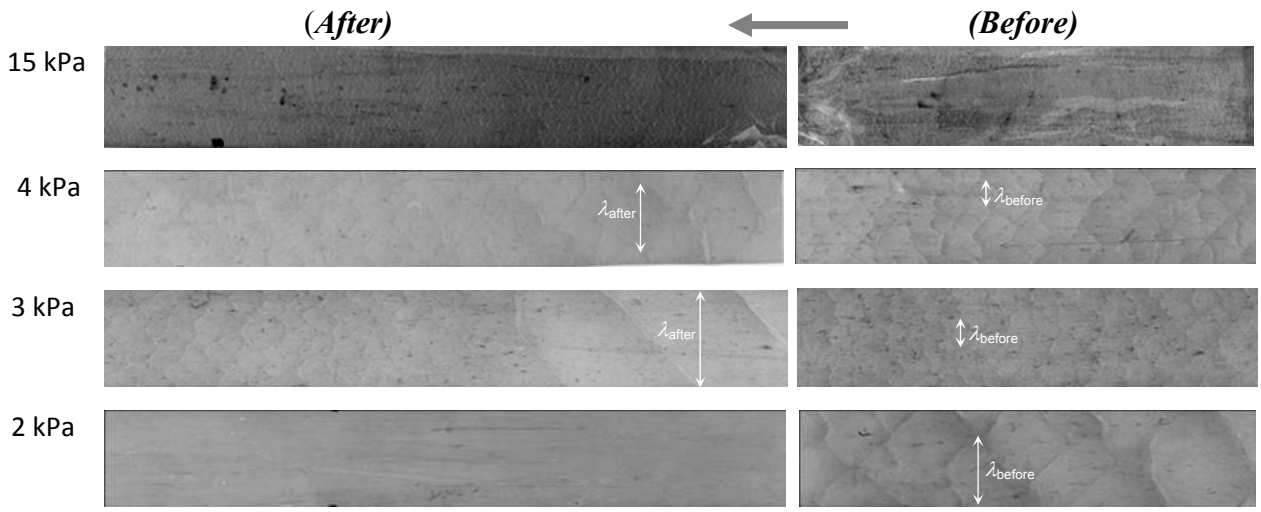

Figure 6.3 Smoked foil measurement showing the cellular structure of the detonation before and after the passage of the porous walled tube in stoichiometric $C_2H_2 + 2.5\ O_2$ mixtures at different initial pressures.

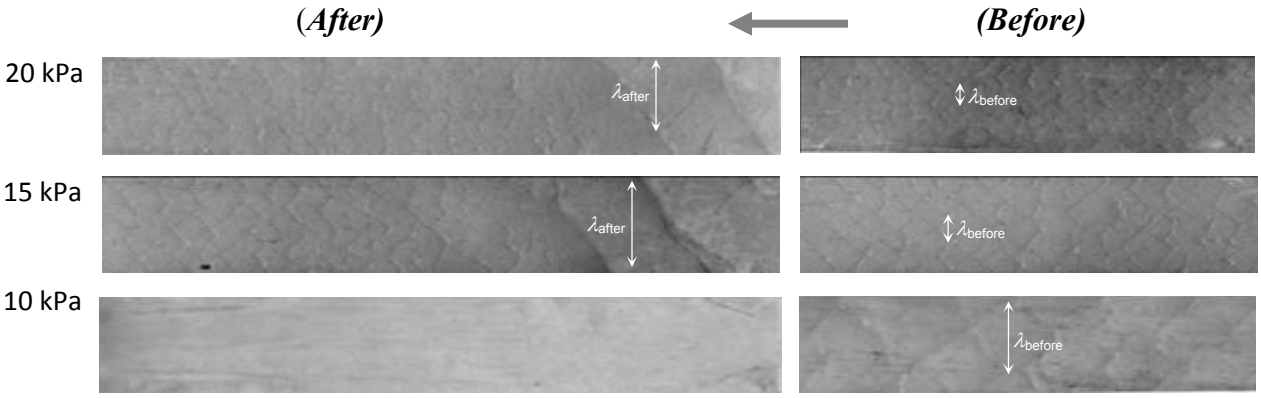

Figure 6.4 Smoked foil measurement showing the cellular structure of the detonation before and after the passage of the porous walled tube in stoichiometric $C_2H_2 + 2.5\ O_2$ +70% Ar mixtures at different initial pressures.

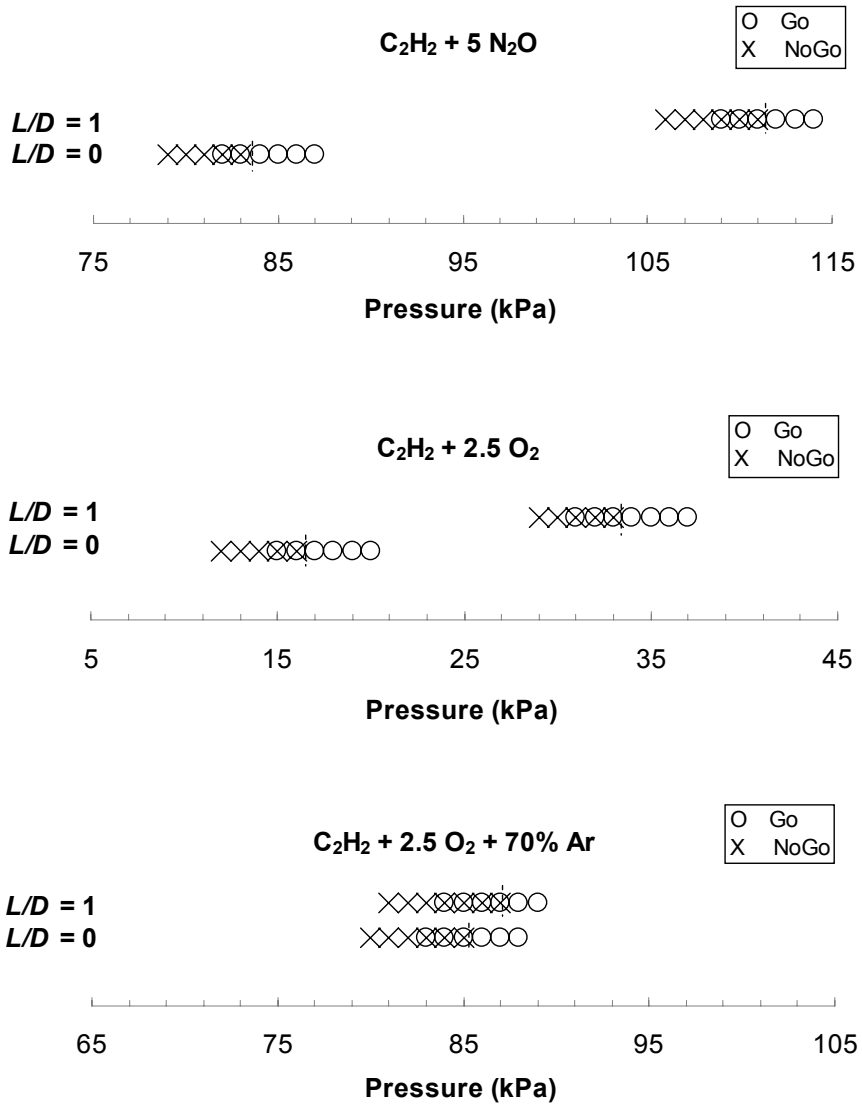

Figure 6.5 Go/No-go plots as a function of initial pressure for the three combustible mixtures.

Critical tube diameter experiments were then carried out with the porous material inserted on the tube wall, close to the exit of the tube. For each combustible mixture and porous media aspect ratio *L/D*, detonation transmission measurements were performed at different initial pressures to vary the sensitivity of the mixture. As in previous work, each experiment was repeated 8 times for each mixture and initial condition to ensure statistical convergence and reproducibility of the results, as well as to identify accurately the critical pressure value above which successful detonation transmission can occur. The critical pressure is defined by the upper limit boundary above which at least 75% of the tests at the same initial condition give a

successful transmission of the detonation wave into the open space. An example of the raw measurement data is given in Fig. 6.5, showing the Go/No-go plot (or successful/unsuccessful transmission) as a function of initial pressure with $L/D = 0$ (non-porous) and $L/D = 1$. In these plots, the overlap between the symbols representing successful (O) and unsuccessful (X) transmission indicates that there is a mixed result among the 8 experimental shots repeated at that particular initial pressure. Such occurrence near critical conditions can be due to inherent sources of experimental variability and is typical for any detonation experiment. In this study of critical tube diameter, the range of uncertainty is not as significant as that of measurements of critical energy for direct initiation or detonation cell size.

Using the data as given in Fig. 6.5, it is possible to identify the critical pressure limit below which the detonation fails to transmit into the open area. Figures 6.6 and 6.7 show the results for the two diameters in all three tested combustible mixtures. For the unstable mixtures, stoichiometric $C_2H_2 + 2.5\ O_2$ and $C_2H_2 + 5\ N_2O$, the results indicate that the porous wall has a significant effect on the critical tube diameter phenomenon. Even with $L/D = 0.50$, there is already a significant increase in the critical pressure.

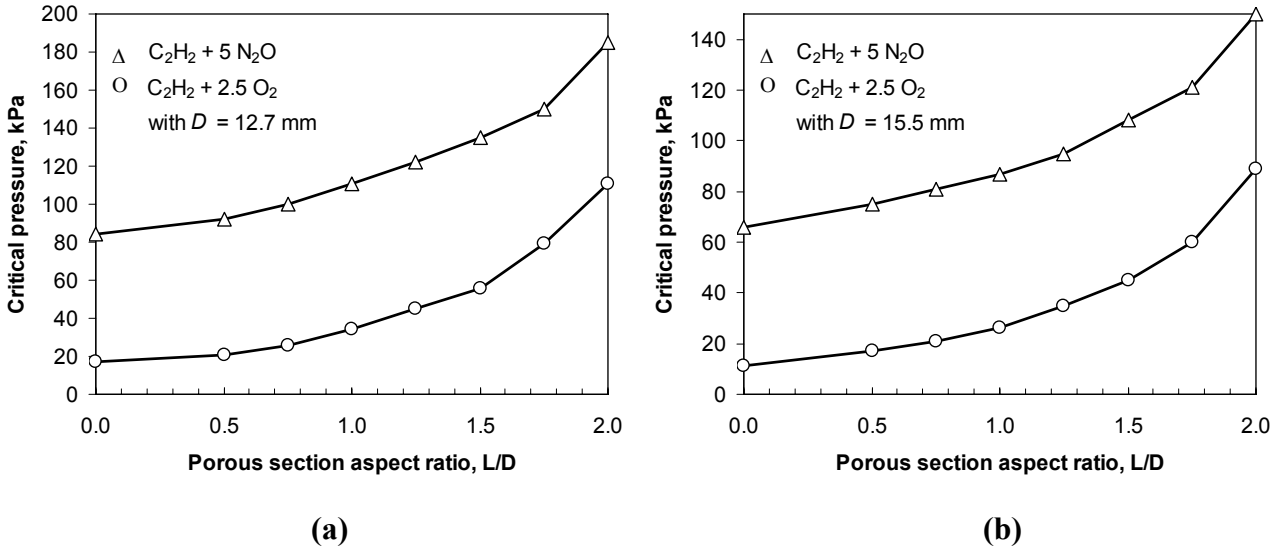

Figure 6.6 The effect of porous walls on the critical pressure for successful detonation transmission for a) $D = 12.7$ mm; and b) $D = 15.5$ mm in two unstable stoichiometric $C_2H_2 + 2.5\ O_2$ and $C_2H_2 + 5\ N_2O$ mixtures.

For the stoichiometric $C_2H_2 + 2.5\ O_2$ with $L/D = 0.50$, the critical pressure increases from 17 kPa to 21 kPa and 11 kPa to 17 kPa for $D = 12.7$ mm and $D = 15.5$ mm, respectively (or

equivalently a difference of about 19% and 35% where % difference is defined by [100% – (x/y · 100%)] with x and y denoting the lower and higher number). A similar increase is also observed for the C_2H_2 + 5 N_2O mixtures with even the lowest $L/D = 0.50$, respectively 8 and 9 kPa increase for D = 12.7 mm and D = 15.5 mm (or a difference of 8.7% and 12%). For these two mixtures, Fig. 6.6 also indicates that increasing the length of the porous walled section causes an exponential increase in the critical pressure limit and eventually no transmission can be observed within the allowable initial pressure for the experiment.

In contrast, the result for the diluted $C_2H_2 + O_2 + 70\%$Ar mixtures shows little dependence on the presence of the porous wall section in the tube. For L/D up to 2.5, the critical pressure limit remains essentially constant (within 1-2 kPa). In other words, the critical condition for successful detonation transmission is not very sensitive to the transverse wave attenuation by the porous media and the flow instability has no major effect on this dynamic parameter of detonation for the diluted mixtures where the detonation wave structure is highly regular. However, for the largest L/D = 3.0 used in this work there is an increase in the critical pressure limit. The dominant mechanism may not be caused by the transverse wave attenuation. This critical pressure increase is likely due to the excessive mass divergence into the porous wall (Radulescu and Lee 2003), leading to the slow distribution of frontal curvature, for long enough L/D, even before the wave emerges into the open area.

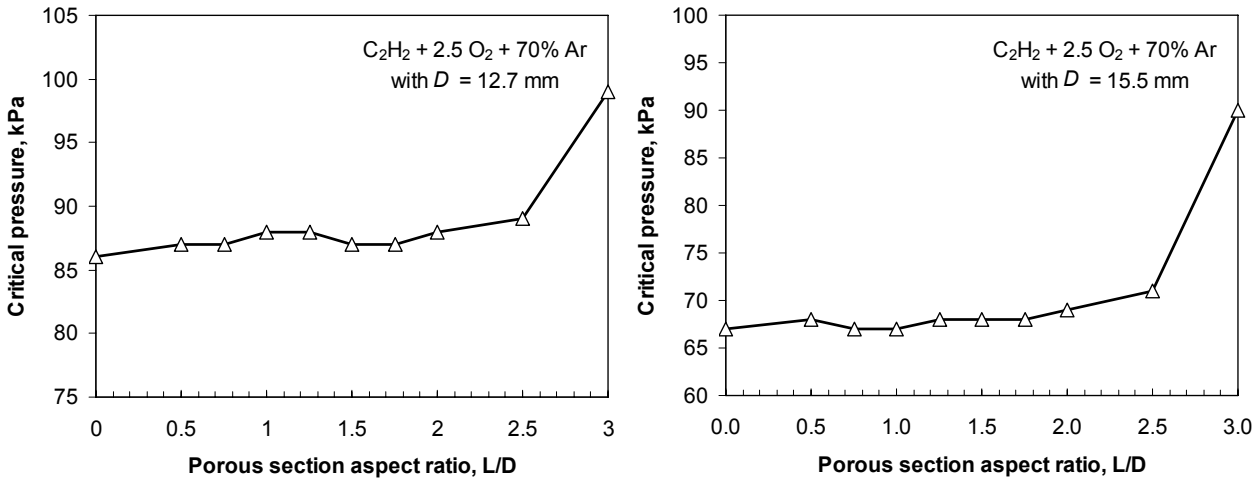

Figure 6.7 The effect of porous walls on the critical pressure for successful detonation transmission for a) D = 12.7 mm; and b) D = 15.5 mm in stable stoichiometric C_2H_2 + 2.5 O_2 + 70% Ar mixtures.

In critical situations where the detonation propagation is prompt to failure, the instability at the cellular front can play an important role on the dynamics of the detonation wave. For unstable mixtures with highly irregular cellular detonation front, it is postulated that the detonation propagation or transmission into the open area relies on the instabilities at the front, i.e., the transverse waves (Lee 1996). The present experiment provides support of this conjecture. For the undiluted C_2H_2 + 2.5 O_2 and C_2H_2 + 5 N_2O mixtures, considered unstable, the attenuation caused by the porous media suppressed the front perturbations and the wave, during the diffraction process, fails to re-generate local explosion centers necessary for a successful transmission. In contrast, for the argon diluted mixture, more stable and exhibiting a very regular detonation front, the instabilities do not play a prominent role and the failure mechanism is proposed to be dominantly caused by the global curvature. The present results are in good agreement with this line of thought. Unlike the cases with unstable mixtures, a short to moderately long porous wall section is shown to have no immediate effect on the critical tube diameter phenomenon. This is due to the fact that the transverse wave attenuation, once the planar detonation enters the porous wall section and before it emerges into the open, unconfined area, does not modify immediately the global front curvature of the detonation wave. Hence, the critical condition for transmission with and without a porous wall with $L/D < 2.5$ shows little variation. The effect of the porous wall may become significant if its length is large enough to allow the development of frontal curvature due to mass divergence, while the wave is still propagating in the porous walled section, before it emerges into the open area.

6.4 Summary

This work is an experimental study of detonation dynamics aimed at understanding the instability of the front that results in different failure mechanisms in the critical tube diameter phenomenon. Experiments using porous walled tubes were carried out to investigate how a self-sustained detonation propagating in a confined tube transmits into an open space, and to confirm the two postulated mechanism governing the successful transmission or failure in the two different types of mixtures (one with highly regular cellular pattern and the other with highly unstable detonation front).

Using a porous wall section near the exit of the confined tube to attenuate the transverse waves, the effect of instability on the failure mechanism of detonation wave diffraction is illustrated for typical hydrocarbon unstable mixtures. From the present, simple experiment, results demonstrate that for unstable mixtures, the successful transmission relies heavily on the frontal instability to generate local explosion centers. Suppression of instability by the porous media before the detonation emerges into the open space causes a significant increase in critical pressure limit for successful transmission. These results thus confirm the failure mechanism consisting in the suppression of instabilities. For stable mixtures such as those highly diluted with argon, the transverse waves at the front are typically weak and the immediate attenuation of these waves by the porous media does not significantly affect the critical conditions for detonation transmission. The failure during the diffraction is therefore caused by the excessive global curvature above which a detonation cannot maintain its self-sustained propagation. This is also found in the present experiments where for long enough damping sections, the mass divergence through the porous wall has sufficient time to distribute its effect and generate front curvature before the detonation wave emerges into the open space, possibly eventually causing failure inside the porous walled section. The already curved detonation therefore will lead to a different critical condition, i.e., an increase of the critical pressure limit for $L/D > 2.5$.

Chapter 7

Summary and Conclusion

7.1 Summary

In this thesis, the phenomenon of critical tube diameters for gaseous detonations is investigated. Experiments were carried out to show the effect of instability on the critical tube phenomenon and all the present experimental results support the existence of two different postulated failure mechanisms for detonation emerging from a confined tube to an open space. For stable mixtures with highly regular structure, the global curvature resulted from the divergence controls the failure limits. The structure in these stable mixtures were found to be highly regular and follows the ideal ZND model where the detonation propagation relies mainly on the global coupling between the shock and the reaction zone.

For unstable mixtures characterized by an irregular structure with strong interacting transverse waves, local instabilities in the reaction structure generated by flow fluctuation permitted to overcome the divergence and transmission can be sustained through local explosion

centers. As demonstrated by the present experiments, both generation of flow disturbance by small obstacles or the attenuation of transverse waves using porous walled tube can significantly affect the critical condition for successful transmission.

The distinct difference in the failure mechanism between the two kinds of mixtures, confirmed in the present thesis work, can also lead to possible implications on the propagation mechanism of detonation. Only for a very special class of mixture the detonation is mainly sustained by the ZND description where chemical ignition by adiabatic compression behind the shock. For most general combustibles, the mixture is unstable of which the irregular structure must rely on instability to permit sufficiently high burning rate to sustain the propagation of the unstable detonation.

7.2 Conclusion and Future Works

In conclusion, only detonations in a very special class of mixture such as those highly diluted with argon can be well described by the classical ZND model, i.e., in mixtures characterized by regular cellular structures, and the failure is caused by the global decoupling of the reaction zone with the leading shock such as caused by the curvature effect in the critical tube diameter problem. For common hydrocarbon detonations characterized by irregular cell structures and turbulent reaction zones, the ignition mechanism relies on both shock compression and instabilities from compressible turbulent interaction for maintaining the sufficiently high burning rate necessary to sustain the wave propagation. Any situation which causes the suppression of these instabilities will lead to failure or other limits phenomena.

For future works, it is ideal to perform more experiments in order to carry out analysis to look at the statistical nature of the Go/NoGo criterion. Since the present study provides mainly a relative comparison between the perturbed and unperturbed cases to elucidate the effect of instability, it is also desirable in the future study to quantify the amount of perturbations by looking at different turbulent scales generated from the obstacles. The effect of tube geometry, e.g., square or rectangular tube and channel, is another interesting subject to explore. Other measurements using optical diagnostics such as Schlieren photography to visualize the diffracting wave front may provide further evidence regarding the effect of curvature. Lastly, to

come up with a better model in the future work to characterize the detonation structure and predict different dynamic parameters, the effect of instability must be properly taken into account in the theory. While for practical application, new technology can be developed from this consideration of instability by either developing devices to suppress transverse waves instability (such as those concepts used in detonation arrestors) or generate instability to promote detonation initiation and its propagation.

7.3 Contribution to Original Knowledge

The present thesis provides important experimental results clarifying the failure mechanism of detonation in the critical tube diameter problem. The experimental observation agrees well with the previously postulated theory that regular structure mixtures characterized by weak transverse waves and piece-wise laminar reaction zone structure fail due to the global curvature during divergence. Irregular structure mixtures characterized by strong transverse waves and unstable reaction zone fail from the attenuation of instability.

Through the experiments conducted in the present thesis, it is thus demonstrated, in a broader way, that only for very special class of mixtures, the detonation is highly regular approaching the classical ZND model and instability play a small role. The ignition mechanism in common unstable mixtures where detonations are characterized by irregular cellular structure, however, relies strong on the self-generation of instability for maintaining the sufficiently high burning rates necessary for the wave self-propagation. The suppression of these instabilities in any limiting cases will cause the detonation to fail.

References

[1] ANSYS Inc. (2009) *Fluent 12.0 Users' Guide*. Canonsburg, PA.

[2] Austin JM, Pintgen F and Shepherd JE (2005) Reaction zones in highly unstable detonations. *Proc. Combust. Inst.* 30: 1849-1857.

[3] Bach GG, Knystautas R and Lee JHS (1969) Direct initiation of spherical detonations in gaseous explosives. *Proc. Combust. Inst.* 12: 853-864.

[4] Baklanov DI and Gvozdeva LG (1995) Non stationary processes during propagation of detonation waves in channels of variable cross section. *High Temperature* 33(6): 955-958.

[5] Bussing T and Pappas G (1994) An introduction to pulse detonation engines. *AIAA conference paper* No. 94-0263.

[6] Camargo A, Ng HD, Chao J and Lee JHS (2010) Propagation of near-limit gaseous detonations in small diameter tubes. *Shock Waves* 20(6): 499-508.

[7] Chao J, Ng HD and Lee JHS (2009) Detonation limits in thin annular channels. *Proc. Combust. Inst.* 32(2): 2349-2354.

[8] Courant R and Friedrichs KO (1946) *Supersonic Flow and Shock Waves*. Springer-Verlag, NY.

[9] Desbordes D (1988) Transmission of overdriven plane detonations: critical diameter as a function of cell regularity and size. *Prog. Astronaut. Aeronaut.* 11:170-185.

[10] Desbordes D, Guerraud C, Hamada L and Presles HN (1993) Failure of classical dynamic parameters relationships in highly regular cellular detonation systems. *Prog. Astronaut. Aeronaut.* 153: 347-359.

[11] Döring W (1943) On detonation processes in gases. *Ann. Phys.* 43: 421-436.

[12] Dupré G, Peraldi O, Lee JHS and Knystautas R (1988) Propagation of detonation waves in an acoustic absorbing walled tube. *Prog. Astronaut. Aeronaut.* 114: 248-263.

[13] Eidelman S and Grossmann W (1992) Pulse detonation engine: experimental and theoretical review. *AIAA conference paper* No.92-3168.

[14] Erpenbeck JJ (1964) Stability of idealized one-reaction detonations. *Phys. Fluids* 7: 684-696.

[15] Fan HY and Lu FK (2008) Numerical simulation of detonation processes in a variable cross-section chamber. *Proc. Inst. Mech. Eng. Part G: J. Aero. Eng.* 222(5): 673–686.

[16] Fickett W and Davis WC (1979) *Detonation*. University of California Press, Berkeley, CA.

[17] Kailasanath K (2003) Recent developments in the research on pulse detonation engines. *AIAA J.* 41(2):145–159.

[18] Kamenskihs V, Ng HD and Lee JHS (2010) Measurement of critical energy for direct initiation of spherical detonations in high-pressure H_2-O_2 mixtures. *Combust. Flame* 157(9): 1795–1799.

[19] Kaneshige M and Shepherd JE (1997) *Detonation Database*. GALCIT Technical Report FM97-8. California Institute of Technology, Pasadena, CA. (Web page at http://www.galcit.caltech.edu/detn_db/html/db.html)

[20] Kapila AK, Schwendeman DW, Quirk JJ and Hawa T (2002) Mechanisms of detonation formation due to a temperature gradient. *Combust. Theory Model.* 6: 553–594.

[21] Kee RJ, Rupley FM and Miller JA (1989) *A Fortran Chemical Kinetics Package for the Analysis of Gas-Phase Chemical Kinetics*. Sandia National Laboratories report SAND89-8009.

[22] Klein R, Krok JC and Shepherd JE (1995) *Curved Quasi-steady Detonations: Asymptotic Analysis and Detailed Chemical Kinetics*. GALCIT FM 95-04, California Institute of Technology, Pasadena, CA.

[23] Knystautas R, Lee JHS and Guirao C (1982) The critical tube diameter for detonation failure in hydrocarbon-air mixtures. *Comb. Flame* 48: 63-83.

[24] Lee JHS (1984) Dynamic parameters of gaseous detonations. *Ann. Rev. Fluid Mech.* 16: 311–336

[25] Lee JHS (1996) On the critical tube diameter. *Dynamics of Exothermicity* (Bowen, J.R. Ed.), Gordon and Breech Publishers, Netherlands, 321-336.

[26] Lee JHS (1997) Initiation of detonation by a hypervelocity projectile. *Prog. Astronaut. Aeronaut.* 173: 293-310.

[27] Lee JHS (2008) *The Detonation Phenomenon*. Cambridge University Press, Cambridge.

[28] Lee JHS, Knystautas R and Yoshikawa N (1978) Photochemical initiation of gaseous detonations. *Acta Astro.* 5: 971-982.

[29] Lee JHS and Higgins AJ (1999) Comments on criteria for direct initiation of detonations. *Phil. Trans. R. Soc. Lond. A* 357: 3503-3521.

[30] Lee HI and Stewart DS (1990) Calculation of linear detonation instability: one-dimensional instability of planar detonations. *J. Fluid Mech.* 216: 103-132.

[31] Li CP and Kailasanath K (2000) Detonation transmission and transition in channels of different sizes. *Proc. Combust. Inst.* 28: 603-609

[32] Lu FK (2009) Prospects for detonations in propulsion. *Proc. 9th Int. Symposium on Experimental and Computational Aerothermodynamics of Internal Flows (ISAIF9)*, Gyeongju, Korea, September 8-11, Paper No.IL-2.

[33] Matsui H and Lee JHS (1978) On the measure of the relative detonation hazards of gaseous fuel-oxygen and air mixtures. *Proc. Combust. Inst.* 17: 1269-1280.

[34] Mehrjoo N, Portaro R and Ng HD (2014) A technique for promoting detonation transmission from a confined tube into larger area for pulse detonation engine applications. *Propulsion Power Res.* 3(1): 9-14.

[35] Mehrjoo N, Zhang B, Portaro R, Ng HD and Lee JHS (2014) Response of critical tube diameter phenomenon to small perturbations for gaseous detonations. *Shock Waves* 24(2): 219-229.

[36] Mehrjoo N, Gao Y, Kiyanda CB, Ng HD and Lee JHS (2014) Effects of porous walled tubes on detonation transmission into unconfined space. *Proc. Combust. Inst.* 35. In press. doi:10.1016/j.proci.2014.06.031

[37] Mitrofanov VV and Soloukhin RI (1965) The diffraction of multi-front detonation waves. *Soviet Physics-Doklady* 9(12): 1055-1058.

[38] Moen I, Sulmistras A, Thomas GO, Bjerketvedt D and Thibault P (1986) Influence of cellular regularity on the behaviour of gaseous detonations. *Prog. Astro. Aero.* 106: 220-243.

[39] Nicholls JA, Wilkinson HR and Morrison RB (1957) Intermediate detonation as a thrust-producing mechanism, *J. Jet Propulsion* 27: 534-541.

[40] Ng HD and Lee JHS (2008) Comments on explosion problems for hydrogen safety. *J. Loss Prevention Proc. Ind.* 21(2): 136-146.

[41] Ng HD and Zhang F (2012) Detonation instability. *Chap. 3, Shock Waves Science and Technology Library, Vol 6: Detonation Dynamics*, F Zhang (ed.) Springer-Verlag Berlin Heidelberg.

[42] Ng HD, Radulescu MI, Higgins AJ, Nikiforakis N and Lee JHS (2005) Numerical investigation of the instability for one dimensional Chapman-Jouguet detonations with chain-branching kinetics. *Combust. Theory Model.* **9**, 385-401

[43] Oran ES (2005) Astrophysical combustion. *Proc. Combust. Inst.* 30: 1823-1840.

[44] Powers JM (2006) Review of multiscale modeling of detonation. *J. Propul. Power* 22: 1217-1229.

[45] Radulescu MI (2003) *The Propagation and Failure Mechanism of Gaseous Detonations: Experiments in Porous-Walled Tubes*. PhD thesis, McGill University, Montreal, Canada.

[46] Radulescu MI and Lee JHS (2002) The failure mechanism of gaseous detonations: Experiments in porous wall tubes. *Combust. Flame* 131(1-2): 29-46.

[47] Radulescu MI, Ng HD, Lee JHS and Varatharajan B (2002) The effect of argon dilution on the stability of acetylene-oxygen detonations. *Proc. Combust. Inst.* 29: 2825-2831.

[48] Roy GD, Frolov SM, Borisov AA and Netzer DW (2004) Pulse detonation propulsion: challenges, current status, and future perspective. *Prog. Energy Combust. Sci.* 30: 545-672.

[49] San Diego Mechanism web page, Mechanical and Aerospace Engineering, University of California at San Diego (http://combustion.ucsd.edu).

[50] Schelkin KI and Troshin Ya K (1965) *Gasydnamics of Combustion*. Mono Book Corp. Baltimore.

[51] Schultz E (2000) *Detonation Diffraction Through an Abrupt Area Expansion*. PhD thesis, California Institute of Technology, Pasadena, CA.

[52] Shepherd JE (2009) Detonation in gases. *Proc. Combust. Inst.* 32: 83-98.

[53] Shepherd JE, Moen I, Murray S and Thibault PI (1986) Analyses of the cellular structure of detonations. *Proc. Combust. Inst.* 21: 1649–1658.

[54] Shepherd JE, Pintgen F, Austin JM and Eckett CA (2002) The structure of the detonation front in gases. *AIAA conference paper* 2002-0773.

[55] Short M (1997) On the critical conditions for the initiation of a detonation in a non-uniformly perturbed reactive fluid. *SIAM J. Appl. Math.* 57(5): 1242–1280.

[56] Sochet I, Lamy T, Brossard J, Vaglio C and Cayzac R (1999) Critical tube diameter for detonation transmission and critical initiation energy of spherical detonation. *Shock Waves* 9: 113-123.

[57] Strehlow RA and Biller JR (1969) On the strength of transverse waves in gaseous detonations. *Combust. Flame* 13: 577-582.

[58] Strehlow RA (1969) The nature of transverse waves in detonations. *Astro. Acta.* 5: 539-548.

[59] Taylor GI (1950) The formation of a blast wave by a very intense explosion. I. Theoretical discussion. *Proc. R. Soc. London A* 201: 159-174.

[60] Teodorczyk A and Lee JHS (1995) Detonation attenuation by foams and wire meshes lining the walls. *Shock Waves* 4(4): 225-236.

[61] Vandermeiren M and Van Tiggelen PJ (1984) Cellular structure in detonation of acetylene-oxygen mixtures. *Prog. Astronaut. Aeronaut* 94: 104-117.

[62] Varatharajan B and Williams FA (2001) Chemical-kinetic descriptions of high-temperature ignition and detonation of acetylene–oxygen diluent systems. *Combust. Flame* 124(4): 624-645.

[63] Vasiljev AA (1994) Initiation of gaseous detonation by a high speed body. *Shock Waves* 3: 321-326.

[64] Vasil'ev AA (1998) Diffraction estimate of the critical energy for initiation of gaseous detonation. *Combust. Expl. Shock Waves* 34(4): 433-437.

[65] Vasil'ev AA (2012) Dynamic parameters of detonation. Chap. 4, *Shock Waves Science and Technology Library, Vol 6: Detonation Dynamics*, F Zhang (ed.) Springer-Verlag Berlin Heidelberg.

[66] Verreault J and Higgins AJ (2011) Initiation of detonation by conical projectiles. *Proc. Combust. Inst.* 33(2): 2311-2318.

[67] Voitsekhovskii BV, Mitrofanov VV and Topchian ME (1958) Optical studies of transverse detonation waves. *Izv. Sibirsk. Otd. Acad. Nauk SSSR* 9: 44.

[68] Von Neumann J (1942) Theory of detonation wave. *John von Neumann, Collected Works.* Vol. 6. Macmillan, NY.

[69] Wang K, Fan W, Yan Y and Jin L (2013) Preliminary studies on a small-scale single-tube pulse detonation rocket prototype. *Int. J. Turbo Jet Engines* 30(2): 145-151.

[70] White DR (1961) Turbulent structure of gaseous detonation. *Phys. Fluids* 4: 465-480.

[71] Yao J and Stewart DS (1995) On the normal detonation shock velocity-curvature relationship for materials with large activation energy. *Combust. Flame* 100(4): 519-528.

[72] Zel'dovich Ya B (1940) On the theory of the propagation of detonation in gaseous systems. *Zh. Eksp. Teor. Fiz.* 10: 542-568. (in *Tech. Memos. Nat. Adv. Comm. Aeronaut.* (1950), no. 1261)

[73] Zel'dovich Ya B (1980) Regime classification of an exothermic reaction with non-uniform initial conditions. *Combust. Flame* 39: 211–214.

[74] Zel'dovich Ya B, Kogarko SM and Simonov NN (1957) An experimental investigation of spherical detonation in gases. *Sov. Phys. Tech. Phys.* 1: 1689-1713.

[75] Zhang B, Kamenskihs V, Ng HD and Lee JHS (2011a) Direct blast initiation of spherical gaseous detonation in highly argon-diluted mixtures. *Proc. Combust. Inst.* 33(2): 2265–2271.

[76] Zhang B, Ng HD, Mével R and Lee JHS (2011b) Critical energy for direct initiation of spherical detonations in H_2/N_2O/Ar mixtures. *Int. J. Hydrogen Energy* 36: 5707-5716.

[77] Zhang B, Ng HD and Lee JHS (2012a) Measurement and scaling analysis of critical energy for direct initiation of detonation. *Shock Waves* 22(3): 275-279.

[78] Zhang B, Ng HD and Lee JHS (2012b) Measurement of effective blast energy for direct initiation of spherical gaseous detonations from high-voltage spark discharge. *Shock Waves* 22(1): 1-7.

[79] Zhang B, Ng HD and Lee JHS (2012c) The critical tube diameter and critical energy for direct initiation of detonation in C_2H_2/N_2O/Ar mixtures. *Combust. Flame* 159(9): 2944-2953.

[80] Zhang B, Ng HD and Lee JHS (2013a) Measurement and relationship between critical tube diameter and critical energy for direct blast initiation of gaseous detonations. *J. Loss Prevention Proc. Ind.* 26: 1293-1299.

[81] Zhang B, Mehrjoo N, Ng HD, Lee JHS and Bai CH (2014b) On the dynamic detonation parameters in acetylene-oxygen mixtures with varying amount of argon dilution. *Combust. Flame* 161(5): 1390-1397.